

---

# **MODULAR NEURAL MECHANISMS FOR ADAPTIVE SPATIAL BEHAVIOR IN AUTONOMOUS ROBOTS**

---

**Dennis Goldschmidt**

Institute of Neuroinformatics, University of Zurich and ETH Zurich

Bernstein Center for Computational Neuroscience, Third Institute of Physics,  
Georg-August-Universität Göttingen

Submission date: 1st October 2014

Supervisor: Prof. Dr. Tobias Delbrück  
External supervisor: Prof. Dr. Poramate Manoonpong  
External supervisor: Prof. Dr. Florentin Wörgötter

**M.Sc. Thesis in Neural Systems & Computation**



# CONTENTS IN BRIEF

---

<b>1</b>	<b>Introduction</b>	<b>1</b>
<b>2</b>	<b>Neural Mechanisms for Control, Learning, and Memory in Spatial Behavior</b>	<b>5</b>
<b>3</b>	<b>Path Integration &amp; Homing Behavior</b>	<b>13</b>
<b>4</b>	<b>Goal-Directed Vector Navigation</b>	<b>29</b>
<b>5</b>	<b>Modular Neural Architecture for Decision Making in Spatial Navigation</b>	<b>41</b>
<b>6</b>	<b>Discussion</b>	<b>47</b>
	<b>Bibliography</b>	<b>51</b>



# CONTENTS

---

List of Figures	vii
Acknowledgments	ix
Acronyms	xi
List of Symbols	xiii
Abstract	xv
<b>1 Introduction</b>	<b>1</b>
1.1 Motivation	1
1.2 Thesis outline	3
<b>2 Neural Mechanisms for Control, Learning, and Memory in Spatial Behavior</b>	<b>5</b>
2.1 Introduction	5
2.2 Neural Coding	7
2.3 Network Models	8
2.4 Neural Integrators	9
2.5 Synaptic Plasticity & Learning	10
2.5.1 Models of correlation-based learning	11
2.5.2 Models of reward-based learning	11
<b>3 Path Integration &amp; Homing Behavior</b>	<b>13</b>

3.1	Introduction	13
3.2	Neural Basis and Ethology of Path Integration in Insects	14
3.2.1	Compass orientation	14
3.2.2	Odometry	17
3.2.3	Systematic angular errors	17
3.3	Existing Models	18
3.3.1	Mathematical models	18
3.3.2	Neural models	19
3.4	A Neural Path Integration Mechanism for Autonomous Robots	20
3.4.1	Sensory input	20
3.4.2	Head-direction layer	21
3.4.3	Odometric modulation of head-direction signals	21
3.4.4	Memory layer	21
3.4.5	Decoding layer	22
3.4.6	Homing behavior	22
3.5	Experimental Results	23
3.5.1	Fixed-orientation outbound runs	23
3.5.2	Random outbound runs	24
3.6	Discussion	25
<b>4</b>	<b>Goal-Directed Vector Navigation</b>	<b>29</b>
4.1	Introduction	29
4.2	Reward-Based Associative Learning for Goal-directed Vector Navigation	30
4.2.1	Global vector learning	30
4.2.2	Global vector navigation	32
4.3	Experimental Results	33
4.4	Discussion	34
<b>5</b>	<b>Modular Neural Architecture for Decision Making in Spatial Navigation</b>	<b>41</b>
5.1	Introduction	41
5.2	Static Action Choice for Two Goal Types	42
5.3	Experimental Results	43
5.4	Discussion	43
<b>6</b>	<b>Discussion</b>	<b>47</b>
<b>Bibliography</b>		<b>51</b>
<b>A NaviSim</b>		<b>61</b>
<b>B Lpzrobots</b>		<b>63</b>
<b>C AMOS II</b>		<b>65</b>

## LIST OF FIGURES

---

1.1	Closed-loop perception-action system	2
2.1	A generalized scheme of the insect central nervous system	6
2.2	Functional diagrams of an insect neuron and synaptic transmission	7
2.3	The model of a simple additive artificial neuron	8
2.4	Self-excitatory feedback as a mechanism for input integration in neurons	10
3.1	The desert ant, a specialist in path integration	14
3.2	The visual sensors of a fire ant	15
3.3	Polarization vision in insects	16
3.4	Neural anatomy of the polarization vision pathway	16
3.5	Neuronal pathway of polarization vision in the insect brain	17
3.6	Systematic errors in the home vector estimation of desert ants	18
3.7	Architecture of the Neural Path Integration Mechanism.	20
3.8	Example of speed modulation using a gater mechanism with 36 neurons	21
3.9	Neural activities of the PI neurons for an example (random) walk.	22
3.10	L-shaped outbound runs and homing behavior using a path integration mechanism	24

3.11	Density maps of estimated home positions	25
3.12	Reproducing systematic errors of desert ant homing	25
3.13	Homing behavior in the simulated hexapod robot AMOS II	26
3.14	Angular errors with respect to noise levels	27
3.15	Angular errors with respect to number of neurons	27
4.1	Goal-directed vector navigation in desert ants	30
4.2	Goal-directed vector navigation control architecture	31
4.3	Reward-based associative learning circuit	32
4.4	Adaptive vector navigation using path integration and vector learning	33
4.5	Global vector learning results for 0% noise level	36
4.6	Global vector learning results for 5% noise level	37
4.7	Goal success rate and exploration rate averaged over 50 learning cycles	38
4.8	Global vector learning in a dynamic environment	39
4.9	Weights and rates during global vector learning in a dynamic environment	40
5.1	Extended learning circuit for multiple goals	42
5.2	Decision making of blue and yellow goals	44
5.3	Exploration rates, choice probabilities and sum of visits of blue and yellow goals in decision making	45
6.1	A proposed scheme of recursive route learning	49

## ACKNOWLEDGMENTS

---

I am very grateful to Tobias Delbrück for admitting my thesis project as a formal supervisor.

I owe my deepest gratitude to Poramate Manoonpong (Koh) for accepting me as student member of his Emmy Noether Research Group. Throughout this thesis and previous work, Koh's guidance, encouragement and support has shaped my scientific career.

I would like to thank Florentin Wörgötter for giving me the opportunity to visit and work in his Department for Computational Neuroscience at the Third Institute of Physics at the Georg-August-University in Göttingen.

Furthermore, I am also very grateful to Sakyasingha Dasgupta for his guidance during this thesis.

I would like to thank the administrators at the Institute of Neuroinformatics (Lottie Walch), and the Department of Computational Neuroscience (Ursula Hahn-Wörgötter) for helping me with any formal questions and regulations.

My special thanks go to Sofy for always being there for me, and for endless hours of corrections and suggestions for this manuscript.

Finally, I thank my parents and family for personal and financial support throughout all these years.

D. G.



## ACRONYMS

---

CR	Conditioned response
CS	Conditioned stimulus
G	Gater
GV	Global vector
HD	Head direction
HV	Home vector
M	Memory
PI	Path integration
TD	Temporal difference
UR	Unconditioned response
US	Unconditioned stimulus



## SYMBOLS

---

$b$	Bias term
$c$	Integration constant
$f$	Transfer function
$i, j, k$	Indices
$l$	Length
$m$	Motor command
$N$	Number of neurons
$n$	Discrete time step
$Q$	Correlation matrix
$q$	Action choice
$R$	Radius
$r$	Reward
$t$	continuous time instant
$v$	Value function
$w$	Weight vector
$W$	Weight matrix
$x$	Neural activity
$y$	Neural activity

$\alpha$	Angle
$\beta$	Choice probability parameter
$\delta$	Prediction error and temporal difference error
$\delta_{ij}$	Kronecker delta
$\lambda$	Leaking rate
$\mu$	Learning rate
$\phi$	Heading direction
$\tau$	Time constant
$\Theta$	Heaviside function
$\theta$	Home vector angle

## ABSTRACT

---

Although small in size, insect brains are capable of generating complex behaviors, such as navigation. In particular social insects, including bees and ants, exhibit outstanding navigational capabilities. Through a process called path integration, they are able to estimate their current location, which is necessary for them to find their way back to the nest after long-distance journeys. This behavior is achieved by integrating compass cues and through odometry. The spatial information obtained during path integration is used as a scaffold for spatial learning in terms of vector navigation. This thesis introduces a neural path integration mechanism that interacts with a neural locomotion control to simulate homing behavior and associative goal learning as it is observed in insects. The mechanism is applied to a simulated hexapod walking robot, called AMOS II. Input signals from an allocentric compass and odometry are sustained through leaky neural integrator circuits, which are then used to compute the home vector by local excitation-global inhibition interactions. The home vector is computed and represented in circular arrays of neurons, where compass directions are population-coded and linear displacements are rate-coded. A reward-modulated associative learning rule is applied for spatial learning of goal locations. This learning algorithm has been shown to converge to stable solutions even in the presence of external sensory noise. Furthermore, we extended the control architecture for learning of multiple goals and goal-directed action selection. The emergent behavior of the controlled agent does not only show a robust solution for the problem of autonomous robot navigation, but it also reproduces various aspects of insect navigation.

## KURZZUSAMMENFASSUNG

---

Trotz ihrer geringen Größe, können Insektengehirne komplexe Verhaltenweisen steuern, wie z.B. Navigation. Insbesondere soziale Insekten, u.a. Ameisen und Bienen, zeigen erstaunliche Fähigkeiten im Navigieren. Durch die sogenannte Wegintegration können sie ihre aktuelle Position bezüglich ihres Nestes bestimmen, welche notwendig ist, um nach langen Reisen wieder zu ihrem Nest zu finden. Insekten schaffen das, indem sie Kompassrichtungen und gelaufene Distanzen aufsummieren. Diese Information wird außerdem für das räumliche Lernen von Vektoren genutzt. Die vorliegende Masterarbeit beschreibt eine modulare, neuro-inspirierte Steuerungsarchitektur für lernfähige Navigation von autonomen Robotern. Diese besteht aus einem neuro-inspirierten Wegintegrationsmechanismus, welcher mit der Bewegungssteuerung interagiert, um die Navigationsfähigkeiten und das räumliche Lernen der Insekten nachzubilden. Die Steuerung ist auf einen simulierten, sechsbeinigen Laufroboter angewandt worden. Der Mechanismus verarbeitet die Signale eines Kompass und eines Schrittzählers zu einer vektoriellen Repräsentation der aktuellen Position in ringförmig angeordneten neuronalen Netzwerken. In diesen Netzwerken werden Kompassrichtungen von bestimmten Neuronen (Population) und Distanzen durch neuronale Aktivitäten (Feuerrate) kodiert. Die Signale werden über Integrationskreise aufsummiert, welche durch lokal erregte und global hemmende Verbindungen den Positionsvektor berechnen. Eine belohnungsorientierte, assoziative Lernregel wird für das räumliche Lernen von Zielen benutzt. Die Ergebnisse zeigen, dass der Lernalgorithmus zu stabilen Lösungen konvergiert, sogar dann, wenn sensorisches Rauschen vorhanden ist. Außerdem ist es möglich, mehrere Zielpositionen zu lernen, welche der Roboter durch ergebnisgerichtetes Handeln ansteuert. Die präsentierte Steuerungsarchitektur bietet nicht nur eine robuste Lösung für das Problem der Roboternavigation, sondern bildet auch eine Vielzahl von verhaltensorientierten Aspekten nach, welche in Insekten beobachtet werden können.

# CHAPTER 1

---

## INTRODUCTION

---

*"A journey of a thousand miles begins with a single step."*

– Lao Tse (604 B.C. - 531 B.C.)

### 1.1 Motivation

This thesis proposes an implementation of an insect-inspired modular navigation system for artificial agents, such as mobile robots, to efficiently navigate through complex environments. Mobile robots possess sensors to perceive environmental stimuli, and motors to produce actions. Thus, they define a closed-loop perception-action system (Fig. 1.1), in which perceived sensory signals are transformed into a motor response by an internal control unit. Autonomous mobile robots have been developed over the past sixty years (Walter, 1953). They offer potential applications in space exploration, as well as maintenance and evacuation tasks in places which are inaccessible or dangerous for humans. Although engineers have developed sophisticated methods to control these robots, their levels of autonomy are still far from being comparable to those of animals. The field of bio-inspired robotics takes inspiration from animal models to create robotic hardware and control systems (Pfeifer et al., 2007). Therefore, these robots have been established as models for the study of adaptive behavior and its underlying control mechanisms (Beer, 1990; Bekey, 2005; Chiel and Beer, 1997).

One of the most challenging, but nevertheless essential tasks of autonomous mobile robots is to navigate through complex dynamic environments. Navigation is divided into *global* and *local navigation*. Global navigation corresponds to the agent's ability to determine its own position and to navigate using a globally defined, allothetic representation, such as a map. On the contrary, local navigation employs local or idiothetic cues, such as objects in the environment (Franz and Mallot, 2000; Trullier et al., 1997). Most robotic systems focus on

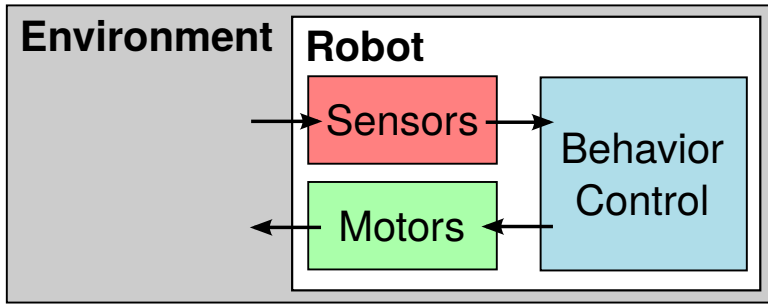


**Figure 1.1** A scheme of a closed-loop perception-action system, such as a mobile robot, interacting with the surrounding environment.

global navigation to solve localization, mapping, and path planning tasks (Borenstein et al., 1997). Throughout the past thirty years, roboticists have proposed solutions to perform these tasks, including potential fields (Khatib, 1985), behavior-based control (Arkin, 1989; Brooks, 1986), occupancy grids (Elfes, 1989), and probabilistic methods, known as Simultaneous Localization and Mapping (SLAM) methods (Durrant-Whyte and Bailey, 2006; Thrun and Leonard, 2008). Despite the success of these approaches, most of them apply high-level sensors (e.g., GPS, laser scanners, and stereo vision) for extensive mapping of the environment, which increases the computational and energy cost of the system and still does not achieve full autonomy of the robotic system.

In contrast, animals navigate their habitat in a fully autonomous, robust and energy-efficient way (Capaldi et al., 1999; Collett and Graham, 2004; Gould, 1998). Neurobiological studies in vertebrates have found multiple neural substrates of internal spatial information, such as hippocampal place cells (O’Keefe and Dostrovsky, 1971), head-direction cells (Taube et al., 1990), and grid cells (Hafting et al., 2005). These findings suggest that animals are capable of building spatial representations of their environment, which are known as cognitive maps (O’Keefe and Nadel, 1978; Tolman, 1948). Not only vertebrates, but also simpler animals, such as insects, exhibit outstanding navigational abilities. For instance, desert ants can directly return to their nests after long foraging journeys through merely featureless environments by integrating their path based on a skylight compass and odometry (Müller and Wehner, 1988; Wehner, 2003). Path integration has also shown to be involved in spatial learning in insects by providing information as a scaffold for vector navigation (Müller and Wehner, 2010). Additionally, insects compensate for accumulating errors, and conflicting or missing information during path integration by using optimal searching patterns, and landmark-guided route navigation (Collett et al., 1998). All of these spatial behaviors do not only rely on sensory information but also on internal states and memories, and are often accompanied by learning mechanisms (Collett et al., 2013; Wystrach and Graham, 2012).

These fascinating capacities for autonomous navigation have inspired many studies on computational models for biomimetic robot navigation based on vertebrates (Burgess et al., 1997; Milford et al., 2004; Prescott, 1996; Strösslin et al., 2005) and invertebrates (Cruse and Wehner, 2011; Franz et al., 1998; Lambrinos et al., 2000; Möller, 2012; Sharpe and Webb, 1998). Nonetheless, the integration of neural control, learning and memory for spatial navigation on an autonomous mobile robot has not yet been fully accomplished.

The main goal of this thesis is to develop a neuro-inspired modular control architecture capable of path integration for homing behavior and spatial learning in vector navigation. This architecture is based on insights from insect navigation and their underlying control mechanisms. Furthermore, it will be implemented on a simulated hexapod walking robot, AMOS II, to model navigational capabilities observed in insects.

## 1.2 Thesis outline

This thesis describes the implementation of neurobiologically inspired mechanisms for insect-like adaptive vector navigation applied to an autonomous robot platform. The structure of the thesis is outlined as follows:

- **Chapter 1** states the motivation behind the thesis: How do animals, in particular, insects generate adaptive spatial behavior and how can possible mechanisms be applied to artificial systems, such as autonomous robots?
- **Chapter 2** describes the computational methods used throughout this thesis. These methods allow for a computationally efficient application of artificial neural networks for control, learning, and memory in a navigating mobile robot, while capturing abstract computational features of the biological system.
- "*How do animals find their way back home?*": **Chapter 3** describes the implementation of a neural mechanism for path integration. This mechanism is applied to a simulated walking robot, and it allows it to estimate its current location with respect to its home position.
- In **Chapter 4**, we describe how path integration is used for place learning and goal-directed vector navigation. To do so, we apply a reward-based associative learning rule to establish the spatial memory of a static global vector connecting the home with the goal location.
- **Chapter 5** integrates the proposed modules into a decentralized, hierarchical architecture for goal-directed action selection. In particular, we extend the learning concept from Chapter 4, such that the robot can learn multiple goal locations and select them during navigation. The robot makes its decision based on previously experienced rewards. We also investigate interactions of the different modules and their emergent behavior.
- Finally, **Chapter 6** provides a concise discussion about the conclusions and implications of this thesis, as well as possible future work.



## CHAPTER 2

---

# NEURAL MECHANISMS FOR CONTROL, LEARNING, AND MEMORY IN SPATIAL BEHAVIOR

---

*"All physical systems can be thought of as registering and processing information, and how one wishes to define computation will determine your view of what computation consists of."*

— Seth Lloyd (1960 - )

### 2.1 Introduction

The vast repertoire of insects' navigational strategies raises the question of how their small brains can generate such complex behaviors. Although it is often assumed that insects primarily respond to external stimuli with a hard-wired reactive behavior, many recent studies show that insects are also capable of higher-order learning and memory-guided behavior.

In order to understand how insects are capable of such behavior, we briefly examine the general structure of the insect nervous system (see Fig. 2.1). This nervous system is composed of a series of paired neural clusters, called ganglia, which are connected thick bundles of axons along the longitudinal axis. The brain (supraesophageal ganglion) consists of three parts called proto-, deuto- and tritocerebra, and it sends efferent signals to the thoracic ganglia, which control leg muscles. The protocerebrum receives afferent signals from the visual system (compound eyes and ocelli), while the deutocerebrum processes inputs from the olfactory system, and from tactile antennal sensing. The tritocerebrum links the brain to the ventral nerve cord. The ventral ganglia (subesophageal, thoracic, abdominal) receive sensory signals from proprio- and mechanoreceptors. In contrast to vertebrates, insects exhibit largely decentralized motor control, e.g., leg movements are generated locally through so-called central pattern generators and fixed reflex circuits. Moreover, many behaviors observed in insects arise from task-specific sensorimotor loops, which perceive sensory signals into appropriate motor re-

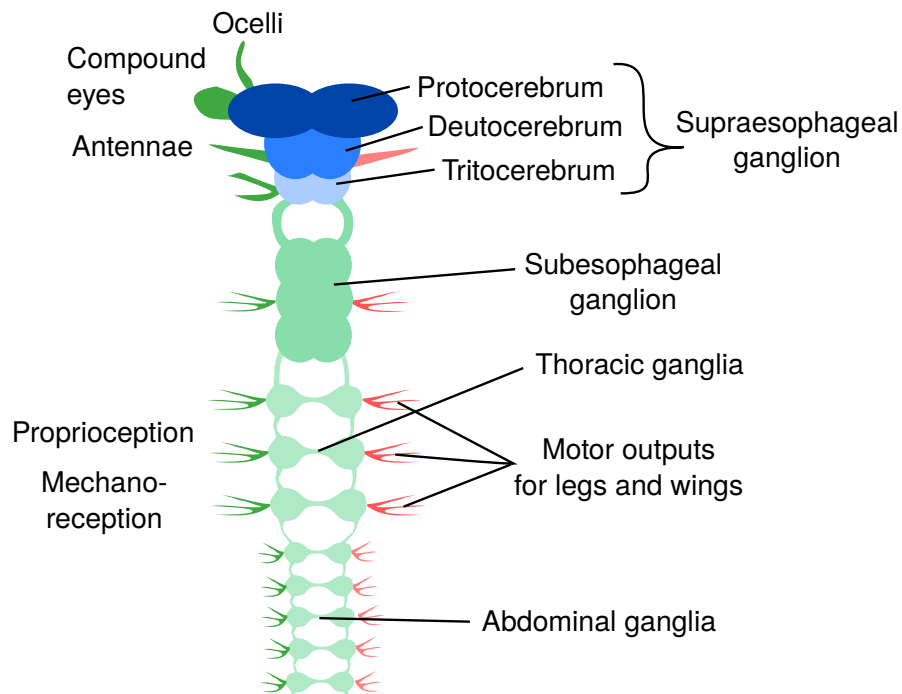


**Figure 2.1** A generalized scheme of the insect central nervous system.

sponses. Note, that these specialized circuits have evolved to solve problems in the ecological context of the animal. The simplicity of the insect nervous system has led to the general belief that the neural architecture of insects can be naively viewed as a system of specialized parallel pathways generating rather simple, stereotyped behaviors. However, many studies on insects' higher-order learning and memory have proved this view to be false. In particular, two integrative higher brain centers have shown to be capable of generating more complex behaviors in insects: the mushroom bodies and the central complex, both located in the protocerebrum.

The *mushroom bodies* are paired, mushroom-shaped protocerebral regions, which consist of three distinct processing layers: the calyx, the pendulculus, and the lobes ( $\alpha$  and  $\beta/\gamma$ ). A mushroom body consists of a large number of densely packed intrinsic neurons, known as Kenyon cells whose fibers run parallel along the body (reviewed in Fahrbach, 2006). At the input layer (calyces), projection neurons connect to the dendrites of the Kenyon cells and provide olfactory input from the antennal lobes. In social insects, they additionally provide visual and mechanosensory input. Kenyon cells are densely packed nerve fibers that project to the lobes, which serve as output region to descending neurons. Many studies have shown that mushroom bodies are involved in olfactory processing, learning and memory (Laurent and Davidowitz, 1994; McGuire et al., 2001; Menzel, 1987; Zars et al., 2000). Additional functions of mushroom bodies have been observed in visual place memory (Mizunami et al., 1998), associative and non-associative plasticity (Szyszka et al., 2008), and locomotor control (Martin et al., 1998). Because of their role in learning and the formation of memories, mushroom bodies have been compared to the vertebrate hippocampus (Strausfeld et al., 1998; Strauss, 2014).

The *central complex* is located at the midline of the protocerebrum and consists of four major areas: the protocerebral bridge, the fan-shaped body, the ellipsoid body, and the noduli. The architecture of the central complex is characterized by parallel pathways arranged in eight columns per hemisphere which are symmetrically interconnected through chiasms (reviewed in Pfeiffer and Homberg, 2014). Most of the input to the central complex is visual and mechanosensory. The main functions of the central complex are related to visual processing (Heinze and Homberg, 2007; Seelig and Jayaraman, 2013), and higher control of locomotion

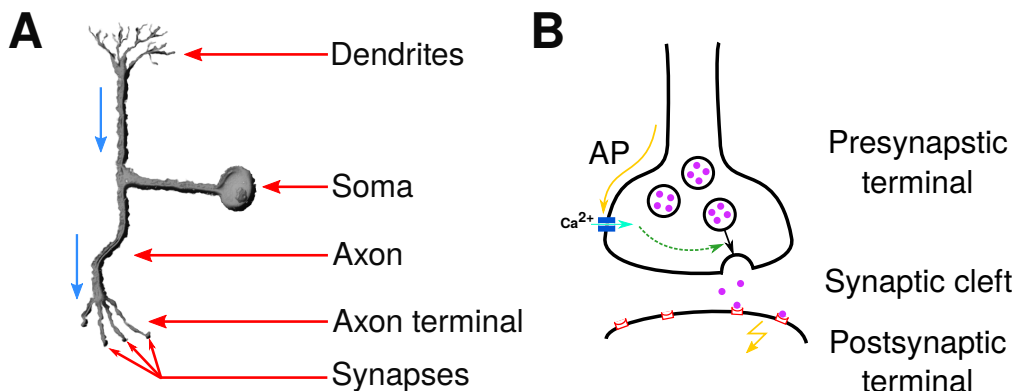


**Figure 2.2** Functional diagrams of an insect neuron and synaptic transmission. A) Most insect neurons are unipolar, i.e., one process extends from the cell body (soma). Incoming signal are received and integrated through dendritic branches. The generated action potential propagates along the axon and terminates in synapses connecting to other neurons. B) Incoming action potentials (AP) at the presynaptic terminal activate the opening of voltage-gated calcium ( $\text{Ca}^{2+}$ ) channels. The influx of calcium ions (cyan-colored arrow) initiates the complex series of events that eventually leads to docking and fusing of synaptic vesicles, a membrane sphere containing transmitter molecules. The release of these molecules into the space between the neurons, called *synaptic cleft*, leads to binding at specific postsynaptic receptors which in response polarize the postsynaptic membrane.

(Strauss, 2002), including turning behavior (Guo and Ritzmann, 2013), orientation (Strauss and Pichler, 1998), step length regulation (Strauss et al., 1992), path integration (Neuser et al., 2008), and visual place learning (Ofstad et al., 2011). A recent study by Weir et al. (2014) showed the role of the central complex in the selection and maintainence of behavioral actions. It has been suggested, that the central complex is comparable to the vertebrate basal ganglia (Strausfeld and Hirth, 2013).

Similar to vertebrates, neurons are the basic components of the insect nervous system, and generate stereotyped electrical signals, called *spikes* or *action potentials*. Neurons are connected to each other through *synapses*, which are specialized structures for signal transmission. Although insect neurons differ in their electrophysiological and morphological properties from their vertebrate counterparts, they share general functional similarities (see Fig. 2.2A). Each neuron receives and integrates incoming signals through tree-like branching processes, known as *dendrites*. They integrate these signals in the cell body (*soma*), and generate spikes. The generation of spikes arises from the dynamics of ionic currents, which flow in and out of the cell through *voltage-gated ion channels* distributed along the cell membrane. Spikes are conducted through an elongated process, called *axon*, which connects to other neurons through the synapses. In the majority of insect neurons, synaptic transmission is achieved by releasing neuroactive chemical molecules in response to incoming presynaptic spikes and the subsequent binding of these molecules to specific postsynaptic receptors at the postsynaptic neuron. This process elicits an response by means of change in membrane potential (see Fig. 2.2B).

## 2.2 Neural Coding

Chapter 1 described how insects navigate through complex environments in an apparently effortless way. In particular social insects of the order *Hymenoptera* are capable of successfully learning and memorizing spatial features of their habitat. Evolution has specialized their brains to perceive, process and represent spatial information. How can a brain occupying only a cubic millimeter of volume encode such complex and manifold information?

The problem of *neural coding* is concerned with this question. There are three different approaches to understanding this problem. Temporal coding is based on the precise timing of single spikes. In this context, spikes are temporally correlated to external stimuli and the brain is made of a neural circuitry that can process this temporal code. Sensory neurons respond to external stimuli with repeated firing of spikes, which increases the mean firing rate.

Rate coding assumes that sensory information is processed through the mean firing rate of neurons (Adrian and Zotterman, 1926). When no relevant external stimuli are present, a neuron exhibits a mean firing rate equal to the baseline rate of its spontaneous activity. On the other hand, when a neuron receives a specific stimulus, its firing rate increases. Rate coding is also relevant for motor control, where incoming spike trains are transformed into contraction force of the muscle. Although rate coding is limited to computations where no precise spike timing and correlations are required, it also conveys information important for central neural processing.

Population coding corresponds to neural encoding of population of neurons (Averbeck et al., 2006; Georgopoulos et al., 1986). This coding scheme was first shown to occur in visual processing (Hubel and Wiesel, 1959), but since then it has also been found in other sensory processing. Population coding assumes that the neural response is defined by a bell-shaped function with a peak response at the neuron's preferred stimuli. This response function is called a tuning curve. Examples for such stimuli-related responses are contrast, orientations, motion direction, and movement speed in the visual system. In insects, the cricket cercal system has a population code for wind directions with a cosine tuning curve. The linear combination of the firing rates across the population is used to infer a vectorial representation of the stimulus source (Jacobs et al., 2008).

### 2.3 Network Models

Network models exploit the computational properties that arise from interactions of massively parallel and distributed neural circuits (Hertz et al., 1991). The first models of artificial neural networks were developed in the twentieth century by McCulloch and Pitts (1943), and Rosenblatt (1962). They assumed that each neuron  $i$  is a simple computational unit (or node) that integrates weighted incoming signals (Fig. 2.3) in order to transmit an "all-or-none" response defined by the Heaviside function:

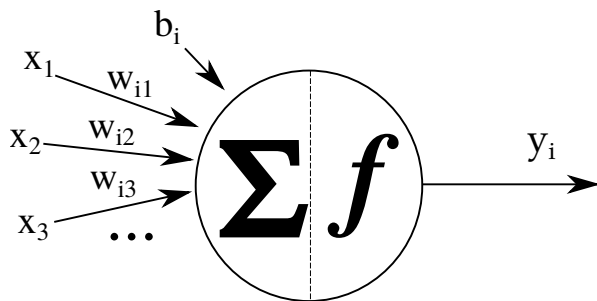


**Figure 2.3** The model of a single additive artificial neuron. It receives and sums the weighted input  $\sum_j W_{ij}x_j$  from  $N$  neurons and a constant bias term  $b_i$ . Within the neuron, two mathematical operations  $\Sigma, f$  process the weighted sum of all inputs to produce the output signal  $y_i$ .

$$\Theta(x) : \mathbb{R} \rightarrow \{0, 1\}, \quad (2.1)$$

$$x \mapsto \begin{cases} 0 & x < 0, \\ 1 & x \geq 0. \end{cases} \quad (2.2)$$

The discrete-time update equations of  $N$  McCulloch-Pitts units are expressed by the one-dimensional map

$$y_i(n+1) = \Theta \left( \sum_{j \neq i}^N W_{ij} x_j(n) + b_i \right), \quad (2.3)$$

where  $x$  are the inputs,  $y$  is the output,  $W$  is the synaptic weight from neuron  $j$  to neuron  $i$ , and  $b_i$  is a constant bias term. It has been shown that these units are equivalent to logic gates (Rosenblatt, 1962). However, this model does not possess internal dynamics. For this reason, models by Caianiello (1961) and Nagumo and Sato (1972) have introduced delay terms to the update equations of the McCulloch-Pitts units. Later works proposed graded responses by applying nonlinear (sigmoidal or hyperbolic tangent) and linear transfer functions (Aihara et al., 1990; Hopfield, 1984), which are biologically relevant characteristics. Using the sigmoidal transfer function  $\sigma(x) = 1/(1 + \exp(-x))$ , Pasemann (1993) introduced a discrete-time neuron model with a self-recurrent connection. This model allows for computationally powerful intrinsic dynamics including hysteresis effects (Pasemann, 1993), chaotic dynamics (Pasemann, 1997), and synchronized chaos (Pasemann, 1999). The simplicity, but yet rich dynamical behavior of map-based neuron models has been successfully applied in several works on neuro-inspired robot control (Manoonpong et al., 2007, 2013; Pasemann et al., 2012; Steingrube et al., 2010).

Throughout this thesis, we apply the network model defined by the discrete-time update equations

$$x_i(n+1) = \sum_{j=0}^{N-1} W_{ij} y_j(n) + b_i \quad (2.4)$$

$$y_i(n) = f(x_i(n)), \quad (2.5)$$

where  $x$  is the weighted sum of input rates and constant bias  $b$ ,  $y$  is the output rate, and  $f$  is the transfer function. In this thesis, linear, rectified linear, and sigmoidal functions are used as transfer functions. Throughout this thesis, we set the step length to  $\Delta t = \frac{n}{t} = 0.1$  s.

## 2.4 Neural Integrators

Temporal integration of sensory signals is a fundamental prerequisite for most cognitive tasks. This computational feature has been observed in electrophysiological recordings of persistent neural activity over period of seconds; for example, in premotor neurons of the oculomotor system of the goldfish (Aksay et al., 2001). Biophysical time constants of single neurons are generally in the range of milliseconds, thus, they cannot explain the observed input integration.

Temporal integration can be achieved by recurrent connectivity in a neural circuit. To show this point we apply a simplified model of a single linear unit with a self-excitatory loop (see Fig. 2.4). Based on the update equations Eqn. 2.4-Eqn. 2.5, the rate update equation is given by

$$y(n) = W y(n-1) + x(n), \quad (2.6)$$

where  $y$  represents the mean firing rate of the integrator circuit,  $W \geq 0$  is the strength of the self-excitatory connection, and  $x$  is an external input to be integrated. For  $W = 0$ , the rate  $y$  is equal to the external input  $x$  and integration does not occur. Rewriting Eqn. 2.6 as a recurrence equation

$$\Rightarrow y(n) = W^n y_0, \quad (2.7)$$

$$= y_0 e^{\ln(W)n}, \quad (2.8)$$

$$\equiv y_0 e^{-\frac{n}{\tau}}, \quad (2.9)$$

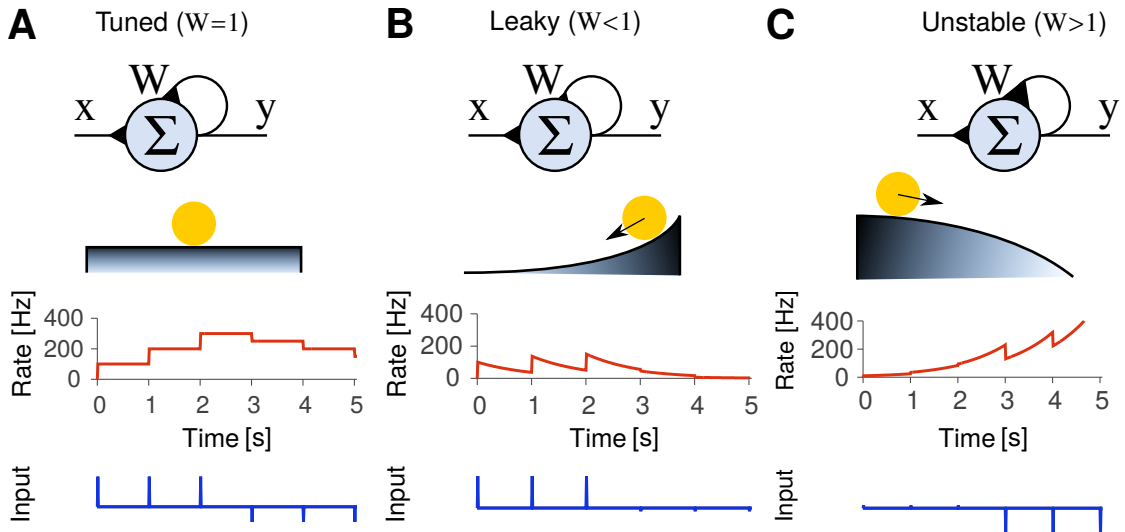


**Figure 2.4** Self-excitatory feedback as a mechanism for input integration in neurons. A) If  $W = 1$ , positive feedback and leakage are balanced and perfect integration is achieved. B) For  $W < 1$ , incoming impulses decay over time and the integration is leaky. C) Diverging behavior of output rates is achieved by  $W > 1$ .

shows that  $y$  decays exponentially with a time constant  $\tau_{\text{int}} = -\frac{1}{\ln(W)} > 0$  for  $W < 1$ . Any external input can only be sustained for a finite amount of time. When  $W > 1$ ,  $y$  diverges exponentially and any external input leads to unstable behavior as the rate  $y \rightarrow \infty$ . For  $W = 1$ , Eqn. 2.6 is equal to

$$\Rightarrow y(n) - y(n-1) = \Delta y(n) = x(n), \quad (2.10)$$

$$\Rightarrow \lim_{\delta t \rightarrow 0} \Delta y = \frac{dy}{dt} = x(t) \Leftrightarrow y(t) = \int x(t) dt, \quad (2.11)$$

and it achieves perfect input integration, which is encoded in the mean firing rate. In this case, there is no information loss (infinite memory). These findings suggest that positive feedback and leakage of neural integrators require fine-tuning of the synaptic weights to solve temporal integration.

## 2.5 Synaptic Plasticity & Learning

*Learning* can be defined as the modification of a behavior through experience. The temporal storage of such modifications is referred to as *memory*. Besides simple non-associative learning forms (habituation and sensitization), animal learning is mainly based on associations of stimuli. In psychology, two forms of associative learning have been observed at a behavioral level: *classical* and *operant conditioning*. Classical conditioning was discovered by Pavlov (1927) in his famous studies on dogs describing the conditioning of a behavioral response to a neutral stimulus. Operant conditioning (Skinner, 1938) describes learning based on rewarded actions. The term *reinforcement* has been coined to describe these behavioral changes: Behavioral responses are increased by positive (rewards) and decreased by negative reinforcement (punishment). These two types of behavioral learning reveal the complexity of how animal nervous systems adapt to certain changes in the environment. The interesting question is how do the behavioral mechanisms described above relate to changes in the brain?

Understanding the underlying biological processes of learning and memory is a central question in neuroscience. It is widely accepted that changes in synaptic efficacy, called synaptic plasticity, underlie learning and memory. Donald O. Hebb (1949) postulated that the synaptic efficacy in the connection of a presynaptic neuron to a postsynaptic neuron is increased when the activities of both neurons are correlated. Thereby, it stabilizes certain causally-driven activity patterns. He argued that the stabilization of activity patterns corresponds to the learning of specific behaviors (Hebb, 1949). With this simple principle, Hebb bridged the gap between synaptic plasticity at the neuronal level and learning at the behavioral level.

### 2.5.1 Models of correlation-based learning

In order to apply synaptic plasticity to the network models presented in section 2.3, we will now formulate mathematical models of the plasticity mechanisms discussed in the previous section. In its simplest form, Hebb's postulate can be expressed as

$$\Delta \mathbf{w} = \mu y \mathbf{x}, \quad (2.12)$$

where the simultaneous activity of  $y$  and  $\mathbf{x}$  leads to positive changes in the weights  $\mathbf{w}$ , which are controlled by a learning rate  $\mu$ . However, synaptic changes do not occur immediately, but over the course of many input patterns  $\mathbf{x}$ . Thus, weight changes are given by the average  $\mu \langle y \mathbf{x} \rangle$ . Eqn. 2.12 can also be expressed in terms of correlations of only the input  $\mathbf{x}$  by replacing  $y$  with  $\mathbf{w}^T \mathbf{x}$

$$\Delta \mathbf{w} = \langle (\mathbf{w}^T \mathbf{x}) \mathbf{x} \rangle = \langle \mathbf{x} \mathbf{x}^T \mathbf{w} \rangle \equiv \mathbf{Q} \mathbf{w}, \quad (2.13)$$

where  $\mathbf{Q}$  is the input correlation matrix. The discretized changes at  $\Delta \rightarrow 0$  describe a first-order linear differential equation

$$\frac{d\mathbf{w}}{dt} = \mathbf{Q} \mathbf{w}, \quad (2.14)$$

which has the solution

$$\mathbf{w}(t) = e^{\mathbf{Q}t} \mathbf{c}, \quad (2.15)$$

where  $\mathbf{c}$  is a constant vector. Because the matrix  $\mathbf{Q}$  is positive definite, the weight vector  $\mathbf{w}$  diverges exponentially. Thus, the standard Hebbian rule (Eqn. 2.12) is unstable, mainly because of autocorrelation terms (Porr and Wörgötter, 2006). To overcome these stability problems of Hebbian rules, subsequent models have proposed modifications to bound weight changes (covariance rule; Sejnowski and Tesauro, 1989), synaptic normalization (BCM rule; Bienenstock et al., 1982 & Oja's rule; Oja, 1982). Porr and Wörgötter (2006) strongly increased stability by replacing the postsynaptic term with an additional predictive input signal.

### 2.5.2 Models of reward-based learning

Reward-based or reinforcement learning is defined as learning through interactions with the environment by means of evaluative feedback, namely reward and punishment. An animal interacting with its environment receives evaluations of past actions, and these influence future actions of the animal ("trial and error"). Consequently, the animal chooses the actions that maximize the total amount of reward over time. First models of reinforcement learning emerged from the field of dynamic programming (Bellman equation; Bellman, 1952). For an extensive review on reinforcement learning, see Sutton and Barto (1998). In the remainder of this subsection, we will focus on mechanistic reinforcement models for neural implementation (Gurney et al., 2004).

Rescorla and Wagner (1972) developed a mathematical model to describe mechanisms in classical conditioning. In this model, the expected reward  $v$  is given by the input stimulus  $x$  multiplied by a weight  $w$

$$v = w x, \quad (2.16)$$

where the weights are updated based on the delta rule

$$\Delta w = \mu \delta x = \mu(r - v)x, \quad (2.17)$$

where  $\mu$  is the learning rate and  $\delta = r - v$  is the so-called *prediction error*, i.e., the error between the actual reward and the predicted one. In terms of classical conditioning,  $r$  can be seen as the rewarding unconditioned stimulus (US) which leads to the innate, unconditioned response (UCR) of the animal.  $x$  is the neutral stimulus to be conditioned (CS). During conditioning, the weight  $w$  increases due to the association of  $x$  and  $r$  and converges towards  $r$  due to increasing activity of  $v$ . Thus, after learning or acquisition, the animal's behavioral response to the CS ( $x$ ) is associated with the reward that the animal is expecting. Similarly, if the CS is now presented without presenting the reward, the weights decrease to zero due to the expected reward  $v$  (extinction). Both, acquisition and extinction learning curves run exponentially towards the steady state solution. Other phenomena in classical conditioning can also be explained in terms of the weight dynamics of the Rescorla-Wagner rule making an impressive, yet simple model of classical conditioning.

It has been shown that animals are able to associate one stimulus with another stimulus which has been associated with a reward. As a result, the so-called secondary stimulus drives the expectation of the reward. This phenomena, termed secondary conditioning, cannot be modelled by the Rescorla-Wagner model. The shortcoming arises from the non-temporal structure of the learning rule. In general, temporal sequences of stimuli that at some point might lead to a reward are intrinsic to the physical structure of the environment. To detect these temporal sequences, the agent must be capable of predicting future rewards. Sutton (1988) formulated a mathematical model based on temporal differences. In this model, predictions  $v(t)$  are not interpreted as predicted rewards at time instant  $t$  as in Eqn. 2.16, but rather as total future rewards expected from  $t$  until the end of the trial

$$\left\langle \sum_{\tau=0}^{T-t} r(t+\tau) \right\rangle. \quad (2.18)$$

and it modify 2.16 into a temporal sum, which estimates predictions of future rewards

$$v(t) = \sum_{\tau=0}^t w(\tau)x(t-\tau). \quad (2.19)$$

For estimating this value, the delta rule can be applied in a modified way, expressed by

$$\Delta w = \mu \delta(t)x(t-\tau), \quad (2.20)$$

where  $\delta$  is the so-called temporal difference error given by

$$\delta(t) = r(t) + v(t+1) - v(t) \equiv r(t) + \Delta v(t+1). \quad (2.21)$$

The temporal difference rule can solve learning problems, where the predictive stimulus and the reward do not occur at the same exact time. Learning determines when the estimate of the value function  $v(t)$  predicts future rewards with the occurrence of predictive stimuli.

This chapter presented neural mechanisms for control, learning and memory in spatial behavior. This biological and theoretical background has been provided in order to develop a neural control architecture for adaptive spatial behavior in autonomous robots. The next chapter describes the implementation of an insect-inspired neural path integration mechanism serving as core module for adaptive vector navigation.

# CHAPTER 3

---

## PATH INTEGRATION & HOMING BEHAVIOR

---

*"Many a trip continues long after movement in time and space have ceased."*

– John Steinbeck (1902 - 1968)

### 3.1 Introduction

Animals have evolved a remarkable diversity of navigational strategies to survive in complex dynamic environments. One of these strategies is to integrate angular and linear ego-motion cues over time in order to maintain a vector representation of their current location with respect to their starting point. This vector representation is called the home vector (HV). The underlying behavior of this process is called path integration (Mittelstaedt, 1983) or dead reckoning, and it is mainly used for homing, i.e., returning back to the home. Path integration has been observed in many animals, including mammals (Etienne and Jeffery, 2004; Mittelstaedt and Mittelstaedt, 1980), avians (Mittelstaedt and Mittelstaedt, 1982; von Saint Paul, 1982), fish (de Perera, 2004), amphibians (Sinsch, 2006), arthropods (Görner, 1958; Zeil, 1998), and presumably cephalopods (Alves et al., 2008; Jozet-Alves et al., 2014). As it was mentioned in previous chapters, social insects, such as ants (Wehner, 2003) and bees (von Frisch, 1965) exhibit outstanding abilities when applying path integration for navigation. Specialists among social insects are desert ants of the genus *Cataglyphis* (Forel, 1902). Even after long journeys consisting of distances up to hundreds of meters, they can pinpoint the location of their nest (see Fig. 3.1). The question is why and how are they capable of such remarkable navigational feat.

One answer certainly lies in the nature of their habitat: The hot, dry and featureless environment of the Saharan area does not allow for strongly landmark-guided or pheromone-guided route navigation. Multiple times they forage from their nest to search for food and bring it back to the nest. Surface temperatures of

approximately 60° C during the day signify the need to return to the nest directly. Thus, their ecological life as Saharan central place foragers favors the existence of a path integration system linked to their nest. In this very specific ecological niche, desert ants have evolved specialized sensory modalities and effectively operating neural systems for path integration. Angular cues are mainly derived from sun- and skylight compass systems, while linear cues are derived from accumulating strides by proprioceptive means and optic flow.

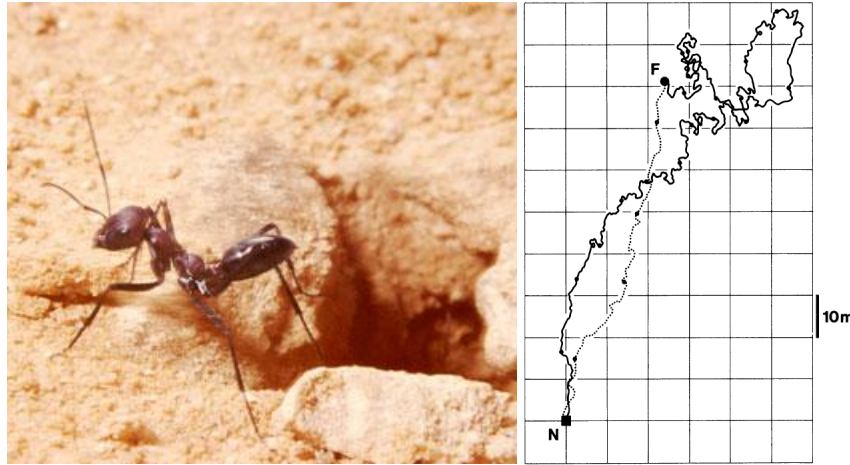


**Figure 3.1** The desert ant, a specialist in path integration. Left: A foraging individual of *Cataglyphis fortis*. Right: Outbound and PI-mediated inbound trajectory of an individual ant, *Cataglyphis fortis*. Black dots are indicating time marks of 60 s. Taken from Müller and Wehner (1988).

The accuracy and robustness of insect path integration makes it a promising prospect for robot navigation. Several previous works have been inspired by path integration in bees or ants for autonomous robot applications (Haferlach et al., 2007; Lambrinos et al., 2000; Zeil et al., 2010). However, since path integration is inherently vulnerable for error accumulation over time, many approaches substitute or recalibrate the path integration measurement by using local views (i.e., landmarks) (Milford and Wyeth, 2008; Mudra and Douglas, 2003).

The goal of this chapter is to develop a neuro-inspired mechanism for path integration and homing and to apply it to an autonomous legged robot. First, we discuss the ways in which animals achieve this behavior. Second, we describe the neuro-inspired mechanism that allows for the modelling of behavioral aspects of path integration as it has been observed in numerous studies of ants and bees. Finally, we apply this neuro-inspired mechanism to a legged robot with the aim to achieve autonomous navigation through complex environments.

## 3.2 Neural Basis and Ethology of Path Integration in Insects

This section describes the sensory modalities and the neural substrates of path integration as well as existing mathematical and neural models. Inspired by these findings, we develop a neuro-inspired path integration mechanism for autonomous robots.

### 3.2.1 Compass orientation

In order to estimate their current position accurately, animals rely on the sensory perception of linear and angular ego-motion cues, and on how these cues are integrated over time. For insects, the main information sources for

allothetic angular cues are the sunlight (Santschi, 1911), the polarization e-vector<sup>1</sup> and the spectral gradients of the skylight. All these cues serve as multiple compasses. Because the sky is virtually at infinite distance, these cues are very reliable for path integration.

**3.2.1.1 Sunlight cues** Early experiments by Santschi (1911), in which harvester ants inverted their homing direction when the light from the sun was flipped by a mirror, indicated the use of sunlight as an orientation cue in insects. Later these first observations were confirmed in various other animals (Kramer, 1952; von Frisch, 1950), including insects and birds. In social insects, photoreceptors of both the insect's compound eyes and, in many species, the three ocelli (lat. *simple eyes*, see Fig. 3.2) can detect changes in light intensity of azimuthal patches (Fent and Wehner, 1985). Information from these two sensors is processed in separate neural pathways and is integrated in more central brain areas (Mizunami, 1995).

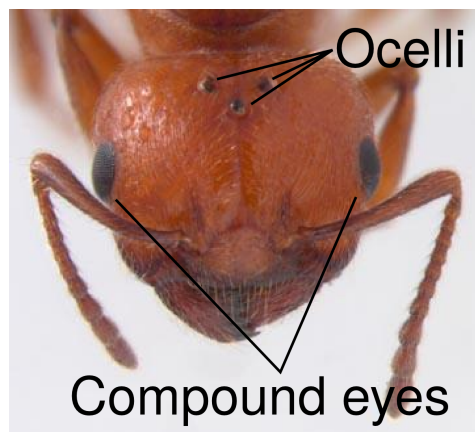


**Figure 3.2** The visual sensors of a fire ant. Compound eyes and ocelli as two separate visual systems of insects.

However, navigation using sunlight information becomes difficult in cases where the sun is concealed by clouds or surrounding objects. Furthermore, higher elevations of the sun lead to larger inaccuracies in the animal's computation of the azimuthal orientation. Thus, a more reliable source of orientational cues is needed to ensure accurate and robust navigation. Insects, like other arthropods, use polarization vision, besides sunlight, as an additional cue.

**3.2.1.2 Polarization cues** Insect vision massively exploits electromagnetic properties of the celestial light. Besides the luminance coming directly from the sun, the polarization pattern of scattered light across the sky is used for orientation (see Fig. 3.3A). Indeed, many insects, including bees (von Frisch, 1949), ants (Duelli and Wehner, 1973; Mote and Wehner, 1980), locusts (von Philipsborn and Labhart, 1990), and flies (Gribakin et al., 1979), are capable of perceiving the e-vector orientation of linear polarized light. The e-vector is detected by a small group of special ommatidia located in the dorsal part of the compound eye, the so-called dorsal rim area (DRA) (see Fig. 3.3B). These ommatidia contain two sets of polarization-sensitive photoreceptors with directions perpendicular to each other.

Polarization-sensitive (POL) interneurons in the optic lobe, classified as POL1 in the cricket *Gryllus campestris* (Labhart, 1988), integrate over large portions of DRA receptors. Therefore, they have large receptive fields of more than 60° directed to the zenith (see green-colored area in Fig. 3.3A). Consequently, POL1 neurons act as spatial lowpass filters, which are insensitive to local atmospheric changes of the e-vector pattern.

<sup>1</sup>Linear polarized light is physically described as orthogonal oscillating vectors of the electric and magnetic fields. The so-called e-vector refers to the orientation of the electric field vector in linear polarized light.

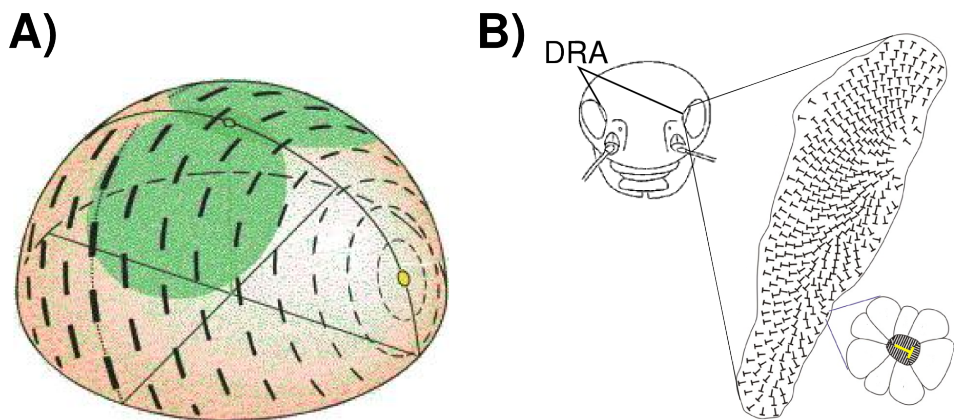


**Figure 3.3** Polarization vision in insects. A) E-vector pattern of linear polarized light in the sky relative to the position of the sun. The green-colored areas depict the visual fields of polarization-visual processing neurons in the optic lobe. Modified from Labhart and Meyer (2002). B) Dorsal rim area (DRA) specialized for linearly polarized light perception. This area contains many polarization-sensitive ommatidia. Modified from Blum and Labhart (2000).

The orthogonal set of photoreceptors in each ommatidium is connected to POL1 neurons in an antagonist fashion<sup>2</sup>. This orthogonality leads to polarization-opponent responses of the POL1 neurons. As a result of this opponency, POL1 neurons exhibit a sinusoidal response function with maxima and minima 90° apart from each other (see Fig. 3.4A). These responses enhance the polarization sensitivity of POL1 neurons and neglect changes in light intensity. POL1 neurons are approximately tuned to one of three preferred e-vector orientations: 10°, 60°, or 130° (see Fig. 3.4B). Based on the activity of this triplet code, the presented e-vector orientation is reliably decoded.

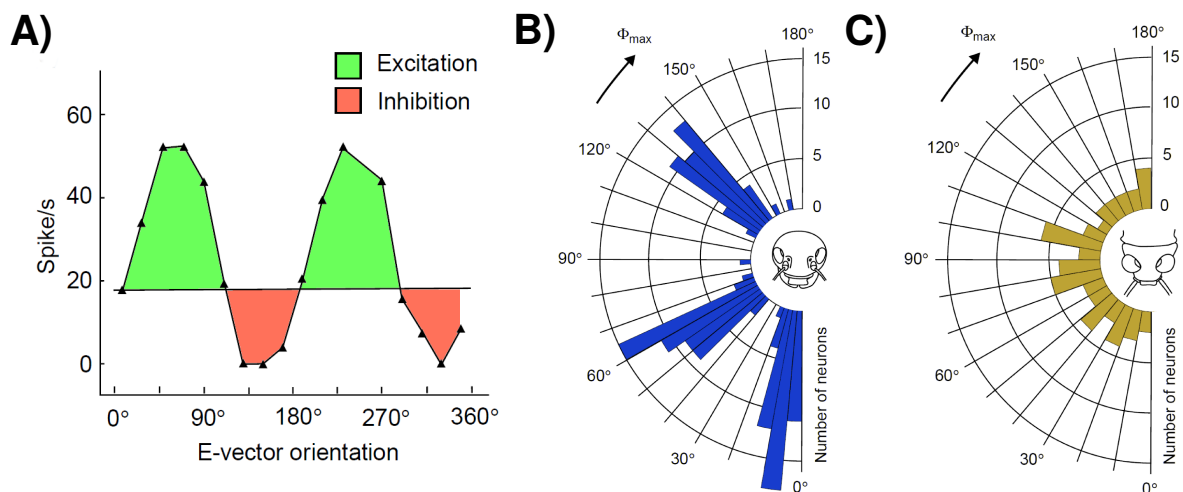


**Figure 3.4** Neural anatomy of the polarization vision pathway in the insect brain (locust). Modified from Labhart and Meyer (2002).

<sup>2</sup>The leading direction excites the cell, while the orthogonal direction inhibits.

POL1 neurons send axonal projections to more central brain areas (see Fig. 3.5), such as the central complex, which also contains polarization-sensitive neurons. These neurons exhibit high activity only for a narrow band of e-vector orientations and, unlike the POL1 neurons in the optic lobe, they show preferred orientations distributed over the full range of possible orientations (see Fig. 3.4C). This suggests that e-vector orientations are represented by a map-like organization of neural responses (population coding) in the central complex, which, in combination with information from sunlight intensity and spectral cues, can be used as a compass (Heinze and Homberg, 2007).

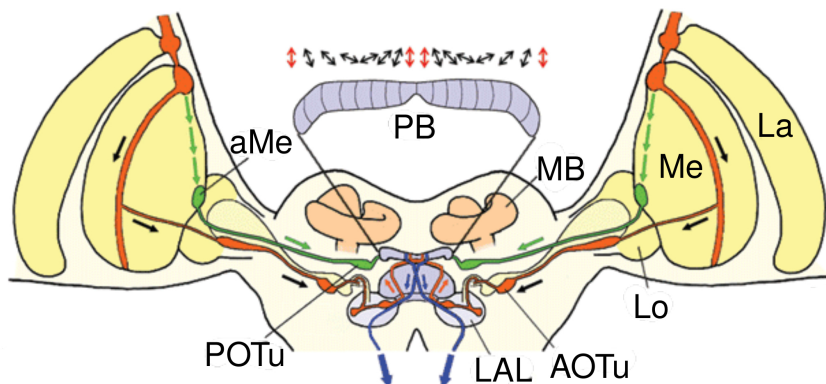


**Figure 3.5** Neuronal pathway of polarization vision in the insect brain. Modified from Homberg et al. (2011).

**3.2.1.3 Time compensation** As the sun moves from east to west throughout the day and changes elevation throughout the year, the insect brain has to compensate for these temporal changes of celestial cues. Several behavioral experiments have shown that insects can compensate for temporal changes of celestial cues (Dyer and Dickinson, 1994; Wehner, 1984). It is generally believed that the so-called circadian clocks, internal mechanisms for time keeping, are responsible for this compensation. In monarch butterflies, these compensation clocks were found in the antennae of the insect (Merlin et al., 2009). In addition, Träger and Homberg (2011) have shown that some types of descending POL neurons project to the thoracic ganglia, and are linearly tuned to particular time-dependent directions.

### 3.2.2 Odometry

Path integration also requires the perception of linear motion cues, because walking speeds of animals are not always constant. Animals can perceive linear motion cues through odometry, i.e., by measuring travelled distances over time. In bees, these cues are provided by the optic flow, i.e., the angular speed of objects in the visual field (Srinivasan, 2014; Srinivasan et al., 1997). In contrast, ants do not use cues from optic flow exclusively, but rather they keep count of their steps (Wittlinger et al., 2006, 2007) using proprioceptive sensors or an efference copy signal of motor commands. In order to compensate for irregular terrains, desert ants also integrate the inclination of path segments (Grah et al., 2005; Wintergerst and Ronacher, 2012). Thus, the resulting home vector shows not the travelled distance, but its ground-projected distance. Inclination signals are provided by proprioceptive gravity sensors located at body and leg joints (Markl, 1962).

### 3.2.3 Systematic angular errors

In a series of experiments involving ants being trained to reach a feeding site through an L-shaped channel, Müller and Wehner (1988) reported the existence of systematic errors in the ant's home vector when released

from the feeder to the test site. These errors were measured as angular deviations from the actual home vector, and they showed that ants misestimate the home position by a short distance located right in front of the actual nest. Thereby they cross the original outbound path (see Fig. 3.6). Similar errors have also been observed in several other species, including bees (Bisetzky, 1957), dogs (Séguinot et al., 1998), and spiders (Görner, 1958).

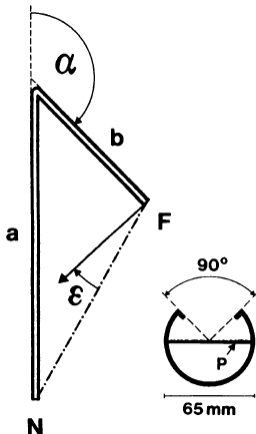


**Figure 3.6** Systematic errors in the home vector estimation of desert ants. Symbols: N, nest; F, food source; a and b, length of first and second segment of the training route, respectively. A cross section of the ant channel shows how the experimenters assured that the ants only rely on path integration. Taken from Müller and Wehner (1988).

### 3.3 Existing Models

This section gives a brief overview of existing mathematical and neural models of path integration with an emphasis on the latter. For a more thorough review, please see Maurer and Séguinot (1995) and Vickerstaff and Cheung (2010).

#### 3.3.1 Mathematical models

Even though path integration has been a subject of investigation since the time of Darwin (Darwin, 1873; Murphy, 1873), it was not until Jander (1957), that a first mathematical model was developed. This model was inspired by observations in the wood ant *Formica rufa*. It assumes that the animal averages angular cues from a light source over time to determine the homing direction. It also assumes that the ant's walking speed is constant and that noise is absent in the system. However, averaging angles over time does not lead to the geometrically correct homing angle (Maurer and Séguinot, 1995). The angles and distances have to be projected to a base reference in order to calculate the correct angle.

Mittelstaedt (1962) proposed a bicomponent model, which uses the projections of individual path segments onto the base vectors of the Cartesian system. The model reciprocally integrates both components<sup>3</sup> of each segment, which are multiplied by the current segment's speed. Although it was developed based on biological

<sup>3</sup>The projections are given by  $dx = \cos(\alpha)$ ,  $dy = \sin(\alpha)$ , where  $\alpha$  is the heading angle, and  $dx$ ,  $dy$  normalized displacements in  $x$  and  $y$  direction.

findings of sinusoidal motor responses in fish orientation (von Holst, 1950), a speed-modulated trigonometric decomposition of orientation cues is not a plausible operation in neural systems.

Several models by Wehner and colleagues (Müller and Wehner, 1988; Wehner and Wehner, 1986) focused on modelling path integration in terms of the observed systematic errors of homing behavior after forced L-shaped runs. These models were based on Jander's model, and they proposed that nonlinear approximations when updating the home vector are the source for the observed systematic errors.

### 3.3.2 Neural models

Touretzky et al. (1993) presented a neural model of path integration based on phasors to represent spatial information (polar vectors). This model computes vector operations using a so-called sinusoidal array: a circular array of neurons that characterizes a sine wave with certain phase. It computes element-wise addition by adding firing rates and vector rotation (Anderson and Van Essen, 1987). Although it was meant to model rodent navigation, the neural representation of orientations and lengths in circular arrays is plausible for invertebrate path integration as well. Wittmann and Schwegler (1995) applied sinusoidal arrays to model ant-inspired path integration. In their model, the home vector phasor ( $r, \theta$ ) is given by the sinusoidal activity pattern  $k_0[r \cos(\theta + \frac{2\pi i}{N})] + b_0$ . This equation is defined for each neuron  $i$ , and  $k_0$  is a gain factor used for speed modulation and  $b_0$  is a constant baseline firing rate. Incoming compass heading signals are converted to the phasor representation and added to the current home vector phasor activity. In order to stabilize the phasor activity, the model suggests recurrent connections within the home vector layer. Homing behavior has been achieved by error compensation with the current heading direction.

The neural model by Hartmann and Wehner (1995) published at the same time as the Wittmann-Schwegler model explains neural path integration as the processing of linear and angular components in separate "chains of neurons". The spatial information about the home vector is represented by a peak of activity travelling according to the differential changes of the linear and angular displacements of the agent. These changes are encoded as firing rates of neurons, which receive input from sensory receptors and project onto the neural chains. Like Müller and Wehner (1988), nonlinear approximations of trigonometric functions in neural responses were proposed to explain the systematic errors in path integration. Free parameters of the model were fitted to the data from Müller and Wehner (1988).

Kim and Hallam (2000) introduced a path integration model with a circular array of neurons, where each neuron has a preferred direction and its activity accumulates with the travelled distance in that direction. The activity pattern of the circular array is transferred to the two neurons encoding the  $x$  and  $y$  positions. The homing direction is computed in a second circular array using inputs from the  $x$  and  $y$  neurons. Homing behavior of their model was tested on a simulated Khepera robot together with a simple controller that facilitates home vector information in a pseudocode. In a more recent paper, Kim and Lee (2011) proposed a similar path integration mechanism without the redundant transformation to  $x$  and  $y$  coordinates.

Bernardet et al. (2008) proposed a model which also accumulates distances in static directions, but uses "neurobiologically plausible" mechanisms to store and decode the home vector. In their model, they integrated allocentric heading and speed cues through a gater mechanism which only transmits heading signals proportional to speed. The sparse activity of the gater is then fed into a much larger layer using probabilistic synaptic transmission. Once these neurons are activated, they stay activated in order to memorize travelled directions. The activity of the memory layer is summed up with respect to the preferred direction and it is connected to the output by a cosine kernel. The home vector angle is given by the maximum argument, and implemented a Winner-Take-All network (see Bernardet et al. (2008) for details). This model was tested in simulation and compared to behavioral data of real ants.

Reviewing the vast literature of models for path integration shows the variability on how this navigational strategy can be computed and embedded into a closed-loop control systems for artificial agents. However, only a few models prove their robustness under realistic conditions, such as in the presence of noise (Benhamou et al., 1990; Cheung, 2014; Cheung and Vickerstaff, 2010). Consequently, path integration models should

be tested in an embodied implementation using mobile robots. Additionally, robotic systems largely benefit from the use of a robust path integration system, because it offers a method for localization using a metric representation. Furthermore, existing models can be categorized by sensory cues (allothetic/ideothetic) used for updating the home vector, as well as the representation of the home vector itself in terms of coordinate systems. This categorization of path integration models is further reviewed in Vickerstaff and Cheung (2010). Both evidence from neurophysiological studies and theoretical studies on noise analysis favor allothetic sensory cues and an integration process by means of static (preferred) heading orientations.

### 3.4 A Neural Path Integration Mechanism for Autonomous Robots

Based on the findings of previous sections, we propose a neural path integration mechanism for autonomous mobile robots. It consists of multiple circular arrays that act as processing layers, where the final layer's activity pattern represents the home vector. Our mechanism applies circular arrays of neurons with population-coded compass information and rate-coded linear displacements. Incoming signals are sustained through leaky neural integrator circuits, and they compute the home vector by local excitatory-lateral inhibitory interactions. Fig. 3.7 shows the architecture of the neural PI mechanism.

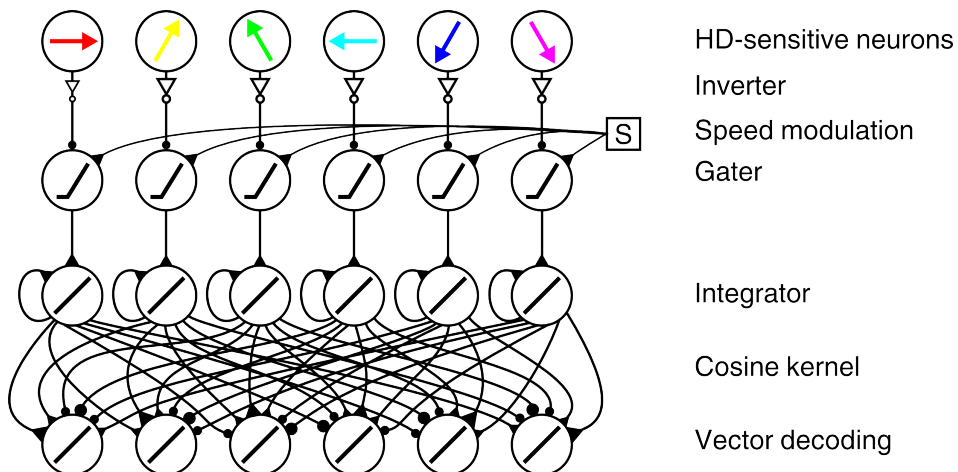


**Figure 3.7** Architecture of the Neural Path Integration Mechanism.

#### 3.4.1 Sensory input

The sensory input to our mechanism consists of two sensors that perceive angular and linear motion cues for path integration. As in social insects, angular cues are derived from an allothetic compass sensor which measures the angle  $\phi$  of the agent's orientation. In insects, this information is derived from the combination of sun- and skylight compass information. Odometry is provided by a speed sensor that measures the speed  $s$  of the agent. For the hexapod robot, the walking speed is computed by accumulating steps and averaging over a certain time window. These step counting signals are derived from the motor signals.

### 3.4.2 Head-direction layer

The first layer of the neural network model consists of head-direction (HD) sensitive cells with activation functions

$$x_i^{\text{HD}}(\phi(t)) = \cos(\phi(t) - \phi_i), \quad (3.1)$$

$$\phi_i = \frac{2\pi i}{N}, \quad i \in [0, N-1], \quad (3.2)$$

where the compass signal is encoded by a cosine response function. The coarse encoding by the cosine ensures high resolution and optimizes information transfer (Eurich and Schwiegler, 1997; Softky, 1996).

### 3.4.3 Odometric modulation of head-direction signals

The second layer acts as a gater mechanism (G), that modulates the neural activity using the walking speed signal  $s$  ( $\in [0, 1]$ ). Thus, it encodes in its activity, the travelled distances of the agent. The gater layer units decrease the HD activities by a constant bias of 1, so that the maximum activity is equal to zero. A positive speed increases the signal linearly. The gater activity is defined as follows:

$$x_i^G(t) = f(\delta_{ij} x_j^{\text{HD}}(t) - 1 + s), \quad (3.3)$$

$$f(x) = \max(0, x) \quad (3.4)$$

where  $\delta_{ij}$  is the Kronecker delta, i.e., the first and second layer are connected one-to-one, and  $f$  is the linear rectifier transfer function. The linear rectifier function only transmits positive signals. Examples of different speed-modulated gater activities are shown in Fig. 3.8. These activities resemble the population code of the combined sky- and sunlight compass systems that reside in the central complex of insects.

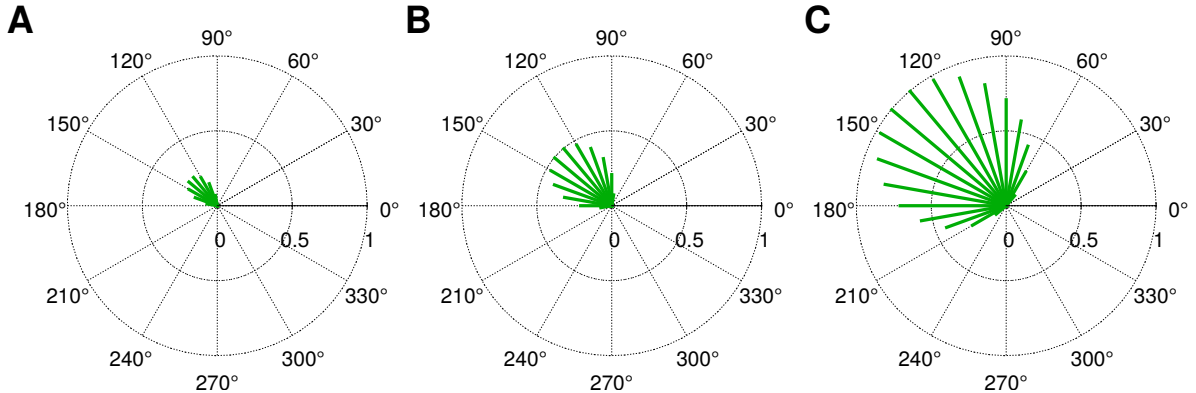


**Figure 3.8** Example of speed modulation using a gater mechanism with 36 neurons. The agent's heading direction is  $\phi = 135^\circ$  and the speed  $s$  is set to A) 0.25, B) 0.5, and C) 1.0.

### 3.4.4 Memory layer

The third layer is the so-called memory layer (M), where the speed-modulated head-direction activations are temporally accumulated through a self-excitatory connection:

$$x_i^M(t) = \delta_{ij} x_j^G(t) + (1 - \lambda) x_i^M(t - 1) \quad (3.5)$$

where  $\lambda$  is a positive constant defined as the integrator leaking rate, which indicates the loss of information over time.

### 3.4.5 Decoding layer

Finally, the fourth layer decodes the activations from the memory layer to generate a vectorial representation of the home vector which is the output of the mechanism (also called PI state):

$$x_i^{\text{PI}}(t) = w_{ij}x_j^{\text{M}}(t) \quad (3.6)$$

$$w_{ij} = \cos(\phi_i - \phi_j) \quad (3.7)$$

where  $w_{ij}$  is a cosine kernel that decomposes the projections of the memory layer activations. The resulting home vector is encoded by the average position of maximum firing in the array (angle  $\theta$ ) and the sum of all firing rates of the array (length  $l$ ). See Fig. 3.9 for example activities of the output layer.

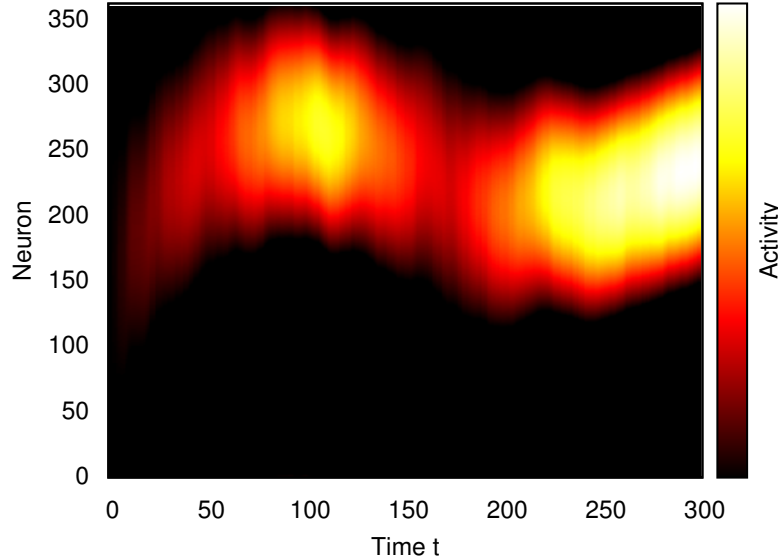


**Figure 3.9** Neural activities of the PI neurons for an example (random) walk.

### 3.4.6 Homing behavior

In order to apply the home vector information for homing behavior, the vector simply needs to be rotated by  $180^\circ$ . The angular error between the current heading direction  $\phi$  and the current inverted home vector direction  $\theta - \pi$  is used for steering the agent towards home. The agent applies homing by error compensation, which defines the motor command

$$m_{\text{hom}} = \sin(\theta - \phi - \pi). \quad (3.8)$$

As a result, positive and negative errors induce right ( $m_{\text{hom}} < 0$ ) and left turns ( $m_{\text{hom}} > 0$ ), respectively, to reduce the error.

### 3.5 Experimental Results

In order to evaluate our path integration mechanism proposed in the previous section, we carry out a series of experiments that test the capabilities and robustness of the mechanism under similar conditions as for animals. In this chapter, as well as for the experimental sections of chapters 4 and 5, we provide results using two different experimental platforms. A two-dimensional simulation *NaviSim*, which consists of a point agent, is used for the main analysis of our control mechanisms (Appendix A). It can efficiently carry out large number of experimental trials, which is required to evaluate our models in a time efficient manner. A second platform is the robotic simulation framework called *Lpzrobots* (Der and Martius, 2012). Advantages of *Lpzrobots* are the open-source availability (<http://robot.informatik.uni-leipzig.de/software/>) and its very accessible interface for simulated robots, including motors and sensors, and environments for robotic simulations (Appendix B). In *Lpzrobots*, we test our navigation control mechanism on the six-legged walking robot *AMOS II*. This robot is biologically inspired, and consists of 19 degrees-of-freedom actuation (three per leg, one body joint) and a multitude of proprioceptive and exteroceptive sensors (see Appendix C for details). Its biomechanical similarities with insects ensures an appropriate embodied model for the study of insect-inspired navigation control.

We test the proposed path integration mechanism in two different experimental setups. First, we let the agent run outbound from an initial home position with two segments of fixed orientations. These runs are referred to as L-shaped runs, where the angle  $\alpha$  defines the angle between the two segments. L-shaped runs are applied under different noise levels to evaluate robustness to noise, and to account for the observed systematic errors observed in the homing behavior of desert ants (section 3.2.3). However, L-shaped outbound runs are not naturally observed in desert ants. Therefore we tested our mechanism in a second experimental setup, in which the agent runs outbound in random orientations. In animals, this foraging behavior serves as an exploration mechanism to find goals in the environment when no indicating stimulus is available.

#### 3.5.1 Fixed-orientation outbound runs

Here we evaluate the capabilities of our mechanism for outbound runs with fixed orientations of the agent. Each run consists of two straight legs in a prefixed direction of  $\alpha_1 = \frac{3\pi}{2}$  and  $\alpha_2 = \pi$ , respectively. Both path segments have the same length of 5. Fig. 3.10 shows the performance of homing behavior for different levels of sensory noise added to the path integration mechanism. For noise levels up to 5%, the path integration mechanism provides reliable estimates of the home position. The estimated home is indicated by the looping behavior of the agent, which results from the sine error compensation for homing (Vickerstaff and Cheung, 2010). In Fig. 3.11, we show the density map of the estimated home position using our path integration mechanism with respect to different sensory noise levels. Increasing noise levels leads to larger uncertainty in determining the current position of the agent. Fig. 3.12 shows that our mechanism is successful in reproducing the systematic errors observed in desert ants (see section 3.2.3). To do so, we fit our model against the desert ant data from Müller and Wehner (1988) using the leaking rate  $\lambda$  of the path integration memory layer as control variable. Values of approximately  $\lambda \approx 0.0075$  is the most consistent with behavioral data. This idea that leaky integration produces systematic errors was previously proposed by Mittelstaedt and Glasauer (1991).

Fig. 3.13 shows the implementation of the L-shaped homing experiment in the simulation framework *Lpzrobots*. Therefore we added our path integration mechanism to the existing locomotion controller of the simulated *AMOS II* hexapod robot to test homing behavior. The homing signal (Eqn. 3.8) controls the speed of the left- and right- sided leg movements, respectively. The video clip of this experiment can be seen at <http://www.manoonpong.com/BCCN2014/homing.wmv>.

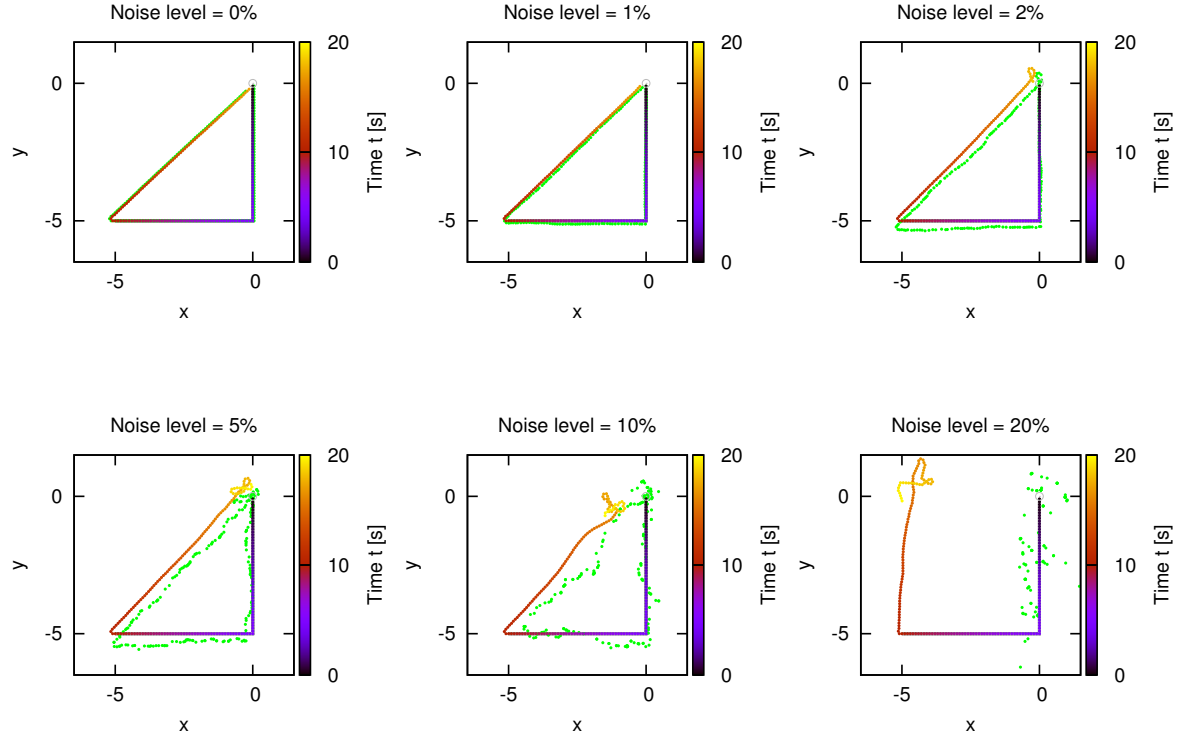


**Figure 3.10** L-shaped outbound runs and homing behavior using a path integration mechanism for six different levels of sensory noise (0, 1, 2, 5, 10, 20%). The multi-colored trajectory is the agent’s position over time. The green-colored trajectory indicates the estimated positions retrieved from the path integration mechanism.

### 3.5.2 Random outbound runs

In order to find resources, animals explore their environments in seemingly randomized patterns. In order to test that our mechanism can also perform under these conditions, we carried out homing experiments after random outbound runs of the agent. Random exploration was achieved by using a gaussian distribution ( $\mu = 0.0, \sigma = 0.15$ ) for the turning rate  $\frac{d\phi}{dt}$ . We tested the performance in terms of angular deviation from actual home with respect to several model parameters: noise, number of neurons. The experiments were averaged over 1000 trials. Fig. 3.14 shows the effect of noise on the performance of path integration. For noise levels up to 5% (equal to  $18^\circ$ ) the angular error is below  $5^\circ$  indicating the robustness of our path integration mechanism. The coarse population coding of heading directions is capable of reducing noise from incoming sensory signals. In Fig. 3.15, we varied the number of neurons in the circular arrays of the path integration mechanism. It shows that the mechanism can produce fairly accurate home vector estimates with 100 neurons. This is again due to the coarse coding of heading directions.

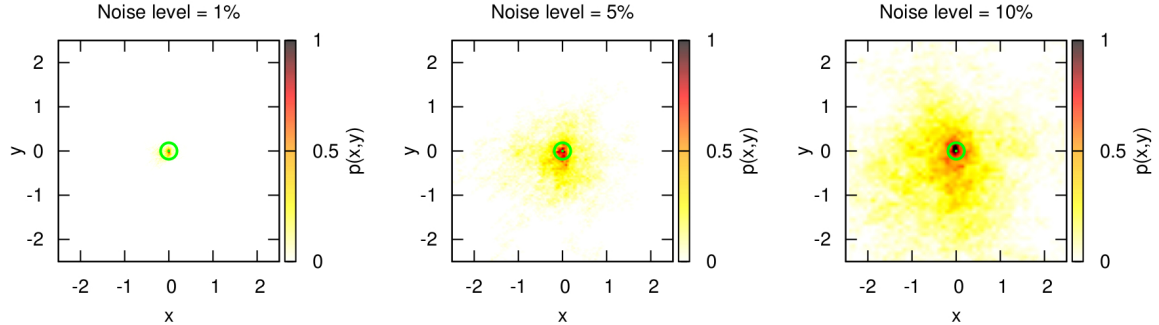


**Figure 3.11** Density maps of estimated home positions using a path integration mechanism for three different levels of sensory noise (1, 5, 10%). The green circle corresponds to the home position with radius  $r_{home} < 0.2$ .

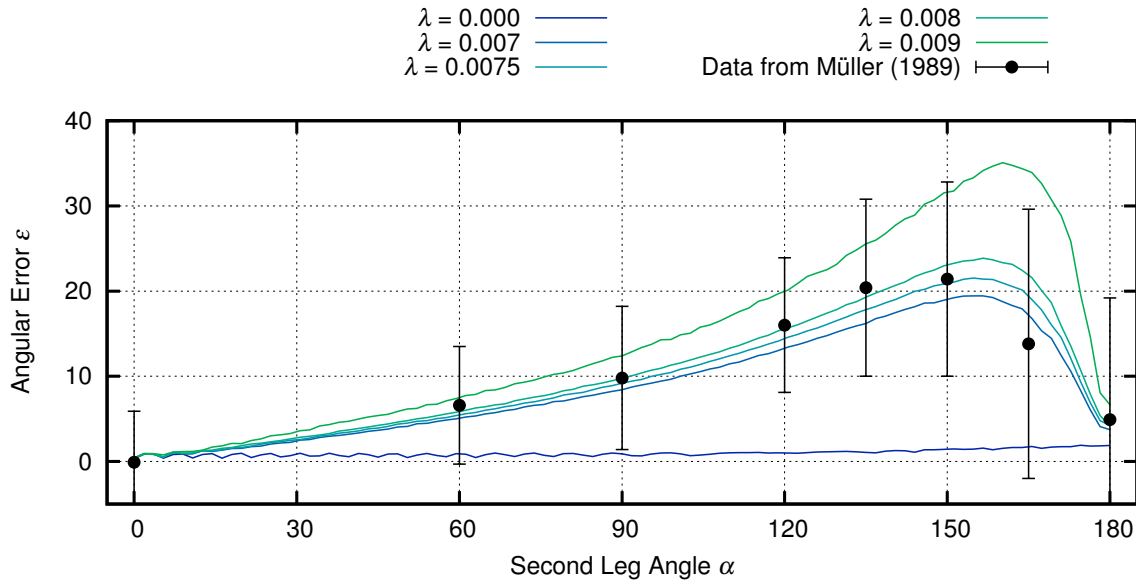


**Figure 3.12** Systematic errors of desert ant homing are reproduced by leaky integration of path segments. The second leg angle  $\alpha$  is varied in  $2.5^\circ$  intervals for the simulation results. A leaking rate of  $\lambda \approx 0.0075$  is used to fit the behavioral data.

### 3.6 Discussion

This chapter presented path integration as a fundamental, but yet challenging computation done by the insect nervous system. It is employed by central place foragers, such as social insects, to locate its current position with respect to its nest. In rodents and other vertebrates, path integration is useful when visual information is abundant. The underlying neural basis of path integration has not been fully understood neither in invertebrates, nor in vertebrates. However, the findings of the main neural pathways, as well as the neural coding of sensory cues required for path integration have shed light onto how animals might process angular and linear self-motion cues.

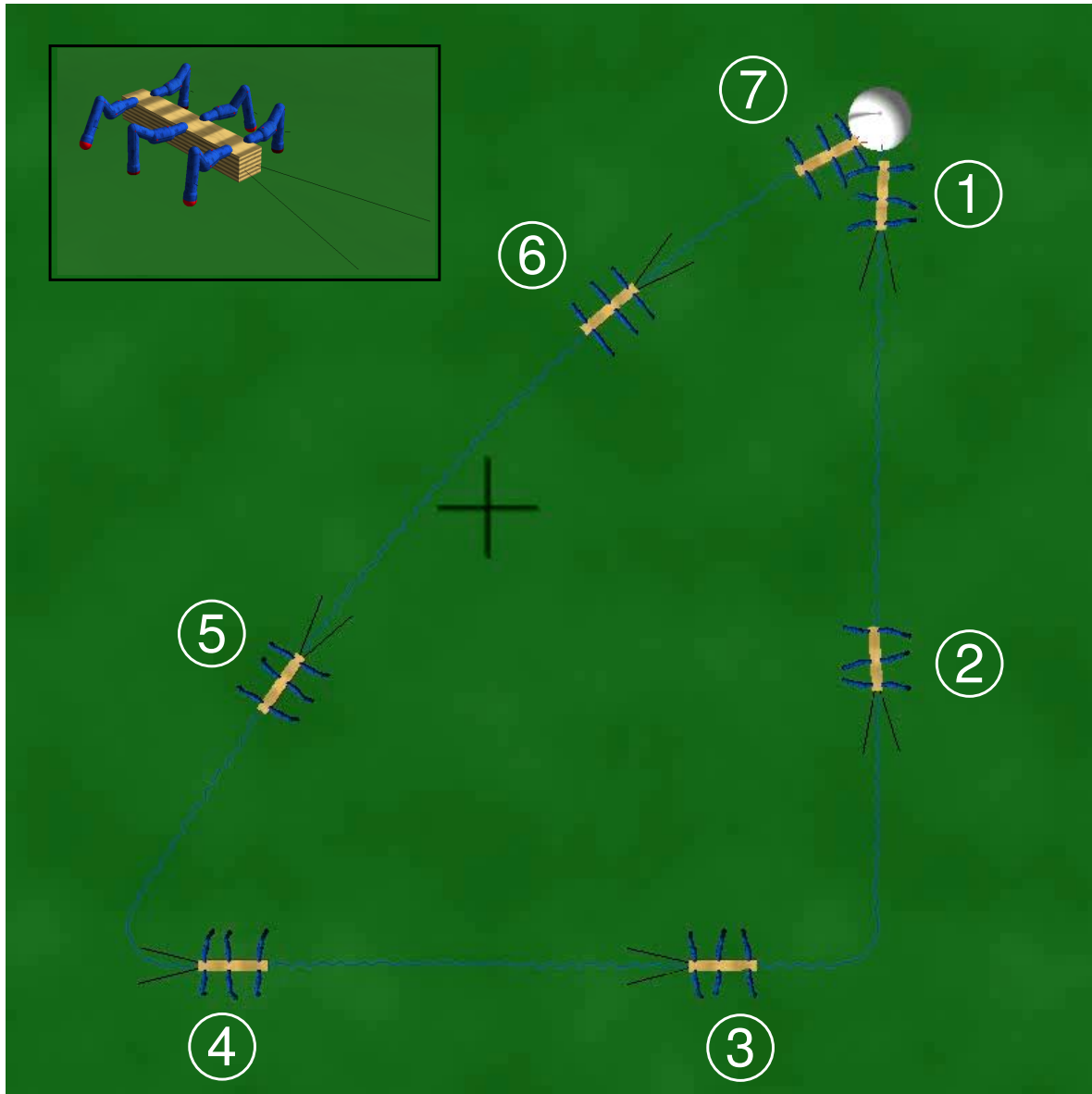


**Figure 3.13** Homing behavior in the simulated hexapod robot AMOS II using the Lpzrobots framework. The robot runs out from its home position (white-colored sphere) in a fixed direction (1-2), before turning right by 90° (3-4). At the end of the L-shaped run, the robot returns to the home position only by using the path integration mechanism (5-7). The in-frame figure in the upper left corner shows the simulated hexapod robot AMOS II.

We presented a neuro-inspired mechanism capable of performing path integration. The mechanism is fed by inputs from an allocentric compass and an odometer providing sensory modalities similar to insects. The home vector is computed and represented in circular arrays of neurons where heading angles are population-coded and linear displacements are rate-coded. This neural representation of spatial knowledge is also found in insects (Heinze and Homberg, 2007; Jacobs et al., 2008). The coarse encoding of orientation using a cosine tuning

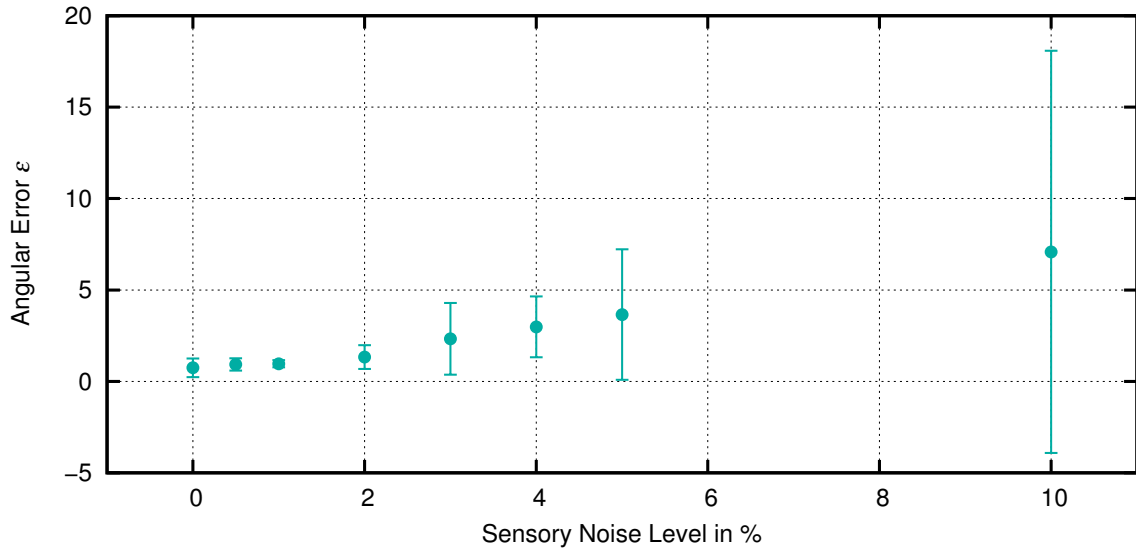


**Figure 3.14** Angular errors ( $\pm$  S.D.) in path integration with respect to sensory noise levels averaged over 1000 trials.

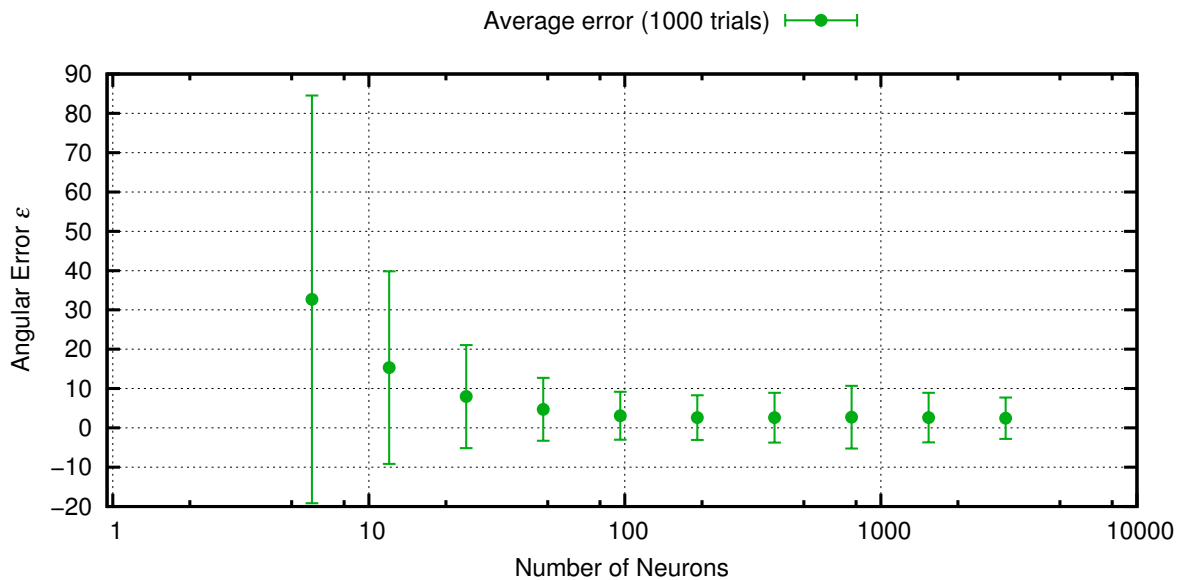


**Figure 3.15** Angular errors ( $\pm$  S.D.) in path integration with respect to number of neurons averaged over 1000 trials.

curve was previously applied by other models (Haferlach et al., 2007; Kim and Lee, 2011). Contrary to these works, our model integrates the walking speed signal as an additive factor, instead of a multiplicative factor. This additive operation is consistent with neural network models. Temporal integration of the speed-modulated head-direction signals is achieved by leaky neural integrator circuits, which are modelled by simple self-recurrent loops. Biologically these recurrent connections can be interpreted as positive feedback within a group of neurons

with the same preferred direction. From a theoretical point of view, we apply this simplified mechanism to avoid random drifts, which are observed in more complex attractor networks (Wang, 2001) proposed in previous path integration models (Touretzky et al., 1993; Wittmann and Schwengler, 1995). Finally, the home vector is computed by local excitatory-lateral inhibitory interactions using a cosine weight kernel. This has been previously applied by Bernardet et al. (2008) and it provides the mathematically correct decomposition of the projections of each direction.

As a result, the mechanism has been shown to successfully navigate a two-dimensional point agent as well as the simulated physical robot back to its home position. The leakage parameter  $\lambda$  provided a single free parameter to successfully fit our model to behavioral data from desert ants (Müller and Wehner, 1988). Other models also provided this evidence (Hartmann and Wehner, 1995; Müller and Wehner, 1988; Wittmann and Schwengler, 1995), however in our model, memory decay is seen as the reason for the observed systematic errors (Mittelstaedt and Glasauer, 1991; Vickerstaff and Cheung, 2010). The extensive analysis of multiple simulations with random foraging revealed that path integration accumulates errors over time. In the presence of noise, the path integration mechanism is still capable of producing accurate estimates of the home vector. We would like to emphasize the application of our mechanism to an embodied legged agent. This experimental platform provides a valid biomechanical model of insects for modelling spatial behavior, such as path integration and homing under similar conditions as in nature. To our knowledge, existing models have not been tested on legged robots.

Besides homing been an obvious behavior mediated by path integration, it may also be involved in spatial learning by acting as a scaffold mechanism. By providing a metric in the environmental space, the path integrator state can be associated to rewarding places, such as feeding sites, and help the learning of visually-guided landmark responses. The role of path integration in goal learning will be described in the next chapter.

## CHAPTER 4

---

# GOAL-DIRECTED VECTOR NAVIGATION

---

” ‘I have no memory of this place at all!’ said Gandalf”

– John Ronald Reuel Tolkien (1892 - 1973), *The Lord of the Rings*

### 4.1 Introduction

The previous chapter introduced path integration as a behavioral strategy to find the straight path back home. More importantly, it provides the animal with a spatial representation of locations, which can be used to form spatial memories (Collett et al., 2013). Indeed, experiments have shown that desert ants are capable of forming such memories by using their path integrator (Collett et al., 1999; Schmid-Hempel, 1984). These memories are interpreted as so-called *global vectors*, because the vector origin is fixed to the nest (Collett et al., 1998). If the ant is forced to take a detour during a foraging trip, the deviation from the global vector is compensated by comparing the global vector with the current path integration state (see Fig. 4.1).

Honeybees employ global vector memories in a unique way. They communicate the acquired location of a flower patch by performing a waggle dance, which encodes distance and direction from the hive to the goal (von Frisch, 1965). The other bees then follow the communicated vector to the flower site (De Marco and Menzel, 2005; Riley et al., 2005). These findings suggest that global vector navigation is a common strategy of social insects, which allows them to navigate their complex environments in a flexible and adaptive way.

The purpose of this chapter is to develop a reward-modulated associative learning rule to learn spatial representations in form of global vectors. The learning rule is embedded in a neural network, that is composed of two input populations (path integration and foraging state) and an output populations (global vector). The

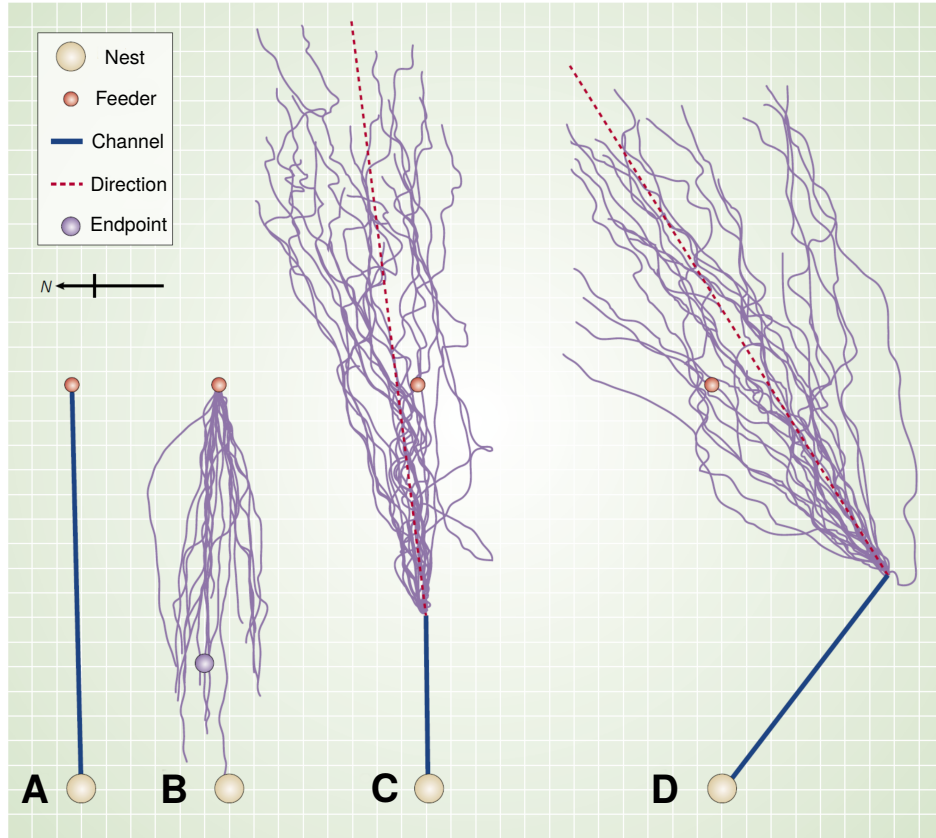


**Figure 4.1** Goal-directed vector navigation in desert ants. (A) Ants were trained to run to a feeder through a fixed channel. (B) Homing behavior of ants. (C) A shorter channel, ants do not change their heading direction. (D) Ants can compensate for detour by subtracting their current path integration state from the global vector memory. Taken from Collett et al. (1999).

learning circuit leads to robust spatial learning of rewarding locations. It can be used to control navigation in a autonomous robot by means of vector navigation.

## 4.2 Reward-Based Associative Learning for Goal-directed Vector Navigation

We propose a reward-modulated associative learning rule for spatial learning of global vectors. The global vector is learned through the association of the path integration state, which represents the conditioned stimulus, and of the reward signal, which represents the unconditioned stimulus. The associated information is used by the agent on future foraging trips to steer towards the rewarding location. The control architecture for goal-vector navigation is shown in Fig. 4.2.

### 4.2.1 Global vector learning

The global vector learning circuit consists of two inputs: the path integration (PI) array and the agent's foraging state (FS), and of an output array, which represents the global vector (GV) to be conditioned (see Fig. 4.3). The GV array has the same number of neurons, i.e., same preferred orientations, as the PI array. In this way, each

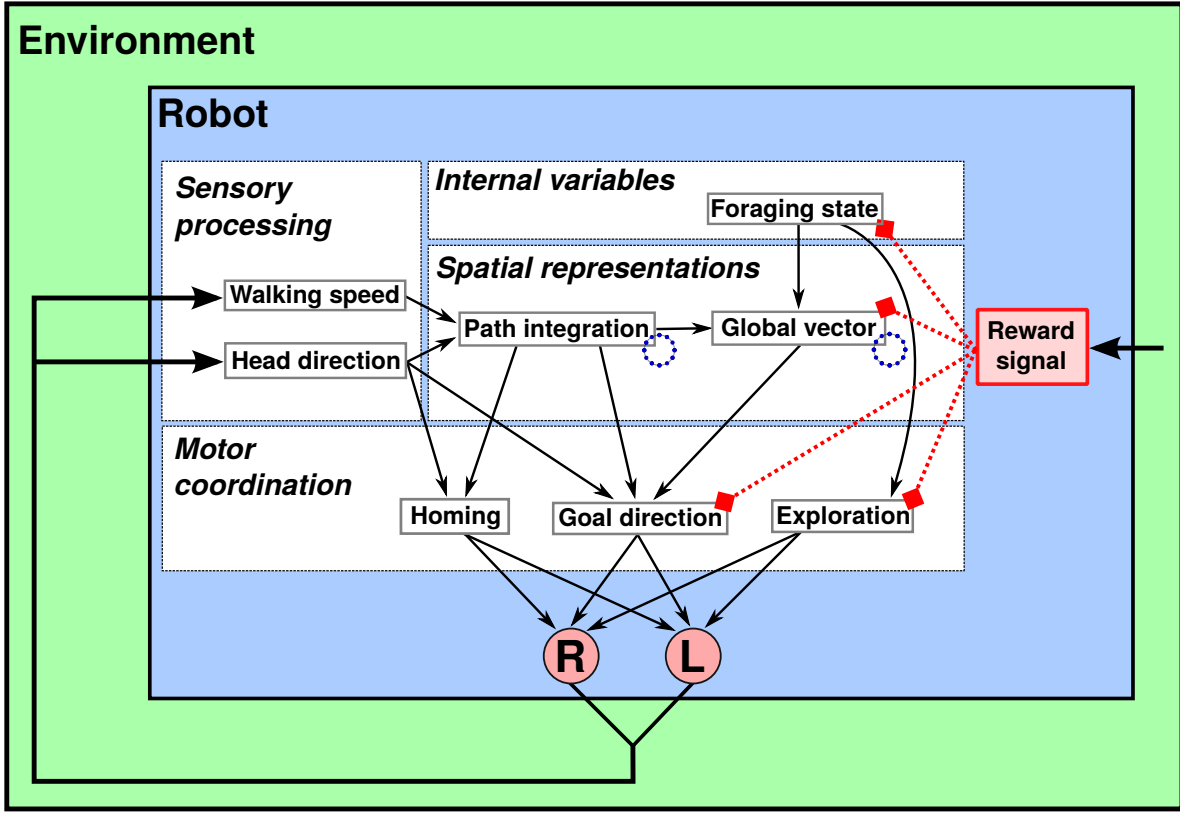


**Figure 4.2** The closed-loop control architecture for goal-directed adaptive vector navigation in autonomous robots.

neuron  $i = 0, 1, \dots, N$  has a preferred orientation of  $\frac{2\pi i}{N}$ . Here, we apply  $N = 360$  neurons for each array. The output  $y_i$  of the learning circuit at time step  $n$  is given by

$$y_i(n) = W_i(n)\xi(n), \quad (4.1)$$

where  $W_i$  are the plastic weights, and  $\xi$  is the foraging state of the agent, i.e.,  $\xi = 1$  if it runs outbound to a goal, and  $\xi = 0$  if it runs inbound to the home. For each trial, the foraging state is set to  $\xi = 1$ , and if the sum of rewards during a trial surpasses a certain threshold, the foraging state switches to  $\xi = 0$ .

We apply a reward-based associative learning rule given by

$$\Delta W_i(n) = \mu r(n)\xi(n)(x_i(n) - W_i(n)), \quad (4.2)$$

$$W_i(n+1) = W_i(n) + \Delta W_i(n), \quad (4.3)$$

where  $r(n)$  is the reward signal,  $x_i(n)$  is the PI activity rate in the direction  $i = \frac{2\pi i}{N}$ , and  $\mu$  is the learning rate. Learning a global vector is achieved by associating  $x_i$  with the reward  $r$ . The reward signal is determined by spatially graded values within the distance of 0.2 to the goal. Mathematically these graded values are defined as

$$r = \begin{cases} 1 - 5d & \text{if } d < 0.2, \\ 0 & \text{else,} \end{cases} \quad (4.4)$$

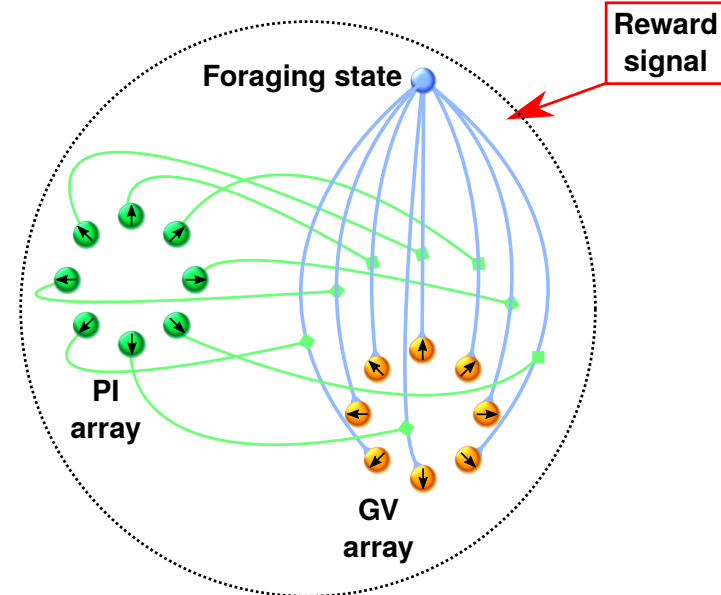


**Figure 4.3** The schematic learning circuit for reward-based associative learning of global vectors. The foraging state  $\xi$  drives the global vector (GV) array. The reward signal acts as a modulatory factor in synaptic plasticity.

where  $d$  is the distance of the agent to a goal. As a result, the vector of the PI state at the rewarding location is imprinted in the weights  $w_i$ . These weights represent the static global vector to the reward location (goal). After returning back home, the agent applies this information to navigate towards the goal.

#### 4.2.2 Global vector navigation

In order to employ the global vector information and efficiently navigate to the goal, the agent needs to coordinate its own actions to steer in appropriate directions. In operant conditioning, appropriate actions are thought to maximize future rewards, and in this way maximize the quantity

$$v(n) = \sum_{i=0}^{t-1} \gamma^i r(i), \quad (4.5)$$

which accumulates the reward with a discount factor  $\gamma = 0.999$ . We use this quantity, known as value function, to control the degree of random foraging, which is expressed by the so-called exploration rate  $\epsilon$ . We define the exploration rate as

$$\epsilon(n) = \exp(-v(n)), \quad (4.6)$$

such that the exploration rate converges towards zero as the agent maximizes the value function, i.e., time-discounted, accumulated reward. This maximization of  $v(n)$  correlates with global vector learning. For random exploration, we sample random values  $\chi$  from a normal distribution

$$\chi \sim \rho(x) = \frac{1}{0.15\sqrt{2\pi}} e^{-\frac{x^2}{2 \cdot 0.15^2}}, \quad (4.7)$$

where the standard deviation  $\sigma = 0.15$  was chosen to achieve optimal searching trajectories.

Learned global vectors are utilized for navigation in the same way as the home vector is utilized in homing behavior. The rate vector  $y$  of the GV array is used to provide a motor command to the agent given by

$$m_{\text{goal}}(n) = \sin(\theta_{GV}(n) - \phi(n)), \quad (4.8)$$

where  $\theta_{GV}$  is the angle to the goal given by the position with maximum activity averaged over the GV array. Additionally, the current position given by the path integrator is applied to compensate any deviations, such as forced detours. This need is illustrated by Fig. 4.4.

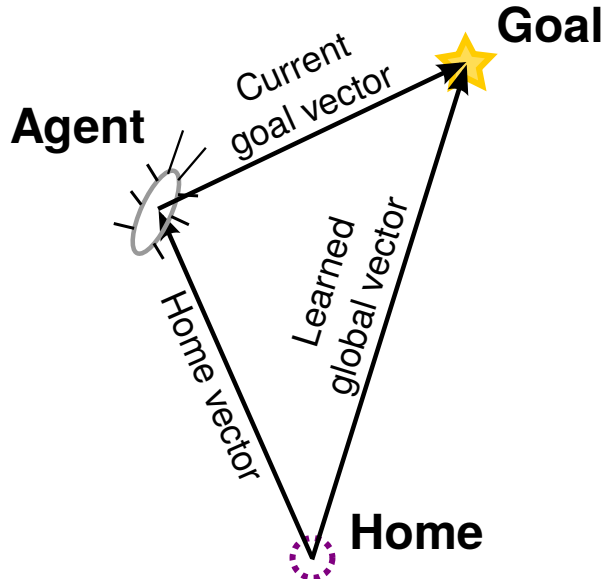


**Figure 4.4** An illustration of adaptive vector navigation using path integration and vector learning. In order to obtain the current direction towards the goal, the current path integrator state needs to be subtracted from the learned global vector.

The final motor command needed to achieve realistic foraging behavior in the agent combines homing, goal-directed and exploratory behavior. The agent is controlled by the motor command

$$m = ||\mathbf{x}||((1 - \epsilon)m_{\text{hom}} + ||\mathbf{y}||\xi(1 - \epsilon)m_{\text{goal}} + \epsilon\chi), \quad (4.9)$$

which combines the output signals for homing  $m_{\text{hom}}$ , goal-directed navigation  $m_{\text{goal}}$ , and exploration  $\epsilon$ . The norm of activities  $||\mathbf{x}||$ ,  $||\mathbf{y}||$  correspond to the lengths of the home and learned global vector, respectively. We apply these norms to achieve the compensation of the current location of the agent as described above.

### 4.3 Experimental Results

We apply the proposed learning algorithm for adaptive goal-directed vector navigation on a simulated agent using NaviSim (see Appendix A). The agent is placed into an environment with randomly distributed goals. Each foraging trip (trial) of the agent consists of an outbound and inbound run with maximum time limit of  $T_{\text{max}} = 500$  time steps respectively. When the outbound time limit is reached, the agent returns back home using path integration. If the agent reaches a goal, it returns home earlier. The agent is reset to the home position if it cannot return to the home position in time. We measured the goal success rate, the exploration rate and the

homing success rate for 100 subsequent foraging trials. The results are shown in Fig. 4.5A. In this experiment, the sensory noise level was set to 0%. Fig. 4.5B shows the density plot of the foraging agent, where visited goals are indicated by green-colored circles. Before learning<sup>1</sup>, the agent's positions are randomly distributed around the nest position (black square). After learning, the agent navigates efficiently between the nearest goal and home. In Fig. 4.5C, we present the PI activity as well as the weights  $W_i$  connecting to the GV array. The green dotted line depicts the average position of the maximum value of both vectors. Note, that each neuron  $i$  corresponds to the preferred direction  $i = \frac{2\pi i}{N}$ .

In order to show the robustness of the learning rule, we applied 5% sensory noise to the path integration inputs. The results are shown in Fig. 4.6, and they demonstrate that the learning rule is able to learn global vectors from noisy PI information. Fig. 4.7 shows the exploration and goal success rate for both 0% and 5% noise levels with respect to the trial number. We averaged these values over 50 learning cycles with randomly generated environments to prove the point that the learning architecture is robust to noise. The agent's exploration corrects misestimated locations, while the exploitation of correct vectors is driven by the experienced reward. Note, that for these experiments, we neglected homing for efficiency. In addition to the acquisition of global vectors, the agent can also forget learned global vectors to learn others. This extinction and reacquisition is shown in Fig. 4.8. In this experiment, the reward signal from the goal locations slowly decays as soon as the vector is learned. When the reward from a certain location is vanished, the exploration rate increases and the agent searches for other goals. The learning rule can quickly establish a global vector, which is shown by the weights  $W_i$  in Fig. 4.9A. The exploration and success rates of this experiment are shown in Fig. 4.9B.

#### 4.4 Discussion

This chapter presented a reward-based associative learning rule for spatial learning using the state of the path integrator. Our results have shown that the robot is capable to learning rewarded locations. The learning algorithm has been shown to be robust, i.e., the robot shows stable goal learning for noise levels up to 5%.

Hoinville et al. (2012) presented a learning circuit for food place memory underlying an existing control architecture for navigation (Cruse and Wehner, 2011). The learning algorithm is comparable to our approach, since it also applies a reward signal to associated spatial coordinates. However, they do not prove that these learning mechanisms can be applied to autonomous robots in a robust way. The spatial representations ( $x$  and  $y$  positions) which are learned in their model are not biologically plausible. Furthermore, the authors mention that their spatial memory once learned, cannot be forgotten. This leads to obvious drawbacks for agents living in a dynamic environment with changing rewards, where reliable food sources with high reward vanish over time. Consequently, their mechanism cannot account for spatial learning and memory as observed in insects. On the other hand, we have shown the extinction of a learned vector by simply decreasing the reward given at the goal. This decrease leads to an increase of the exploration rate. As a result, the agent begins to explore randomly in order to find another goal. This behavior is also observed in insects (Heinrich, 1984; Menzel and Muller, 1996). Insects learn about rewards as described by classical conditioning. In navigational, insects associate spatial cues, as well as local exteroceptive cues, with the presented reward. Exteroceptive stimuli are not considered in our learning model, however, it is possible to include them as additional input to stabilize learning.

It is also worthwhile to mention that the discount factor is the main determinant of the maximum goal distance that can be learned. As a goal location is moved further away from the home, the agent takes longer to travel towards it. Consequently, the value function is decreased, which in turn increases the exploration rate. We argue that insects naturally forage within a certain spatial range, and they have possibly evolved an optimal value function estimation, which is useful to achieve goal learning within this range. Furthermore, landmark-based navigation could guide the agent towards a long-distance goal. This point will be further discussed in Chapter 6.

<sup>1</sup>Here defined as the time interval, where the exploration rate is larger than 0.5.

Although the presented learning rule and control mechanisms are relatively simple, they are capable of generating flexible and efficient behavior for navigation. These findings suggest that even simple modulatory plasticity rules can explain the formation of global vector memories in social insects. In the next chapter, we extend this learning architecture to learn multiple goal locations and achieve goal-directed decision making.

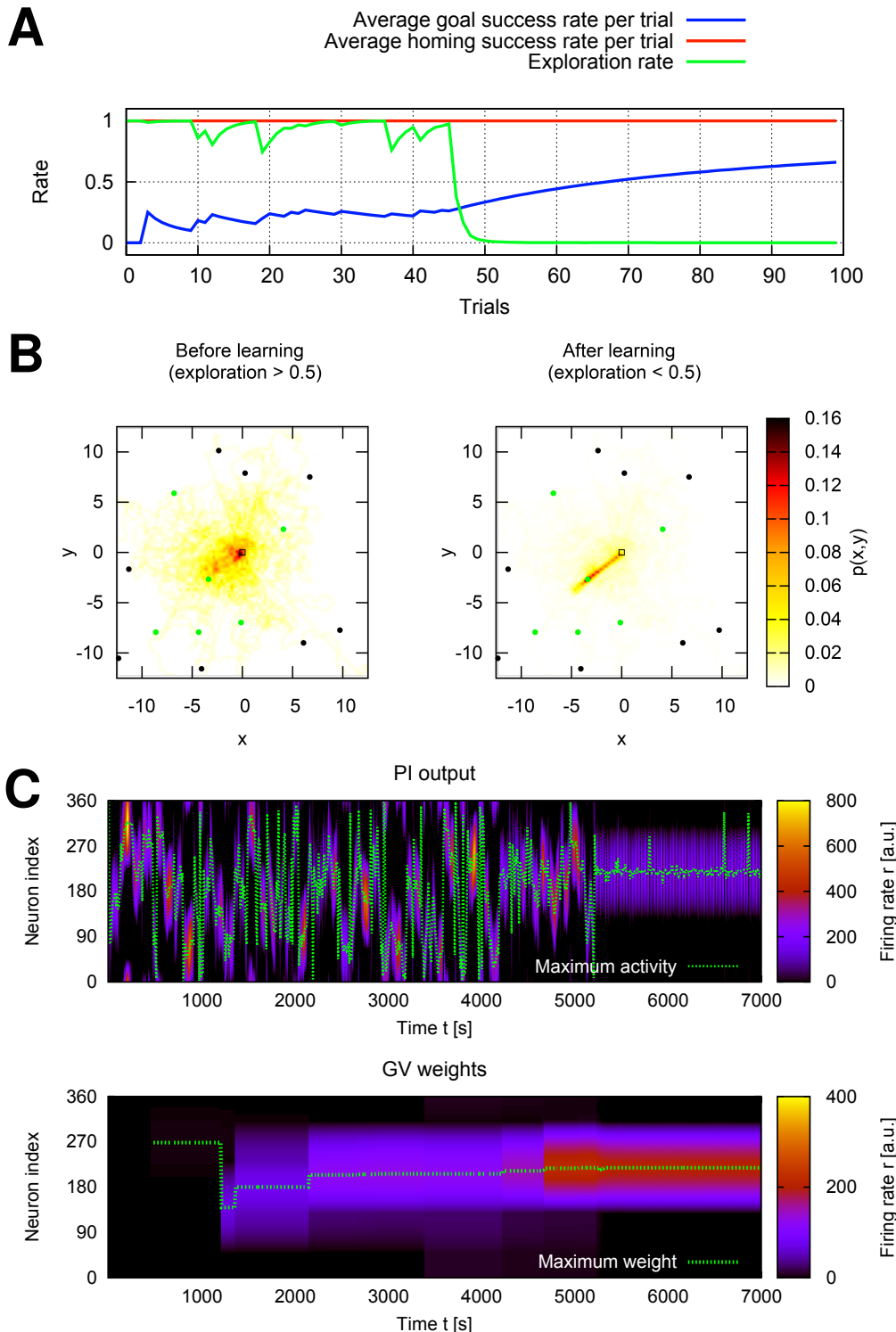


**Figure 4.5** Global vector learning results for 0% noise level. A) Success rates of goal reaching and homing, and exploration rate for 100 learning trials. B) Trajectory density maps before (left) and after learning (right). Visited goals during the experiments are indicated by green circles, while the black circles are the ones not visited by the agent. C) PI activities and GV weights with respect to time.

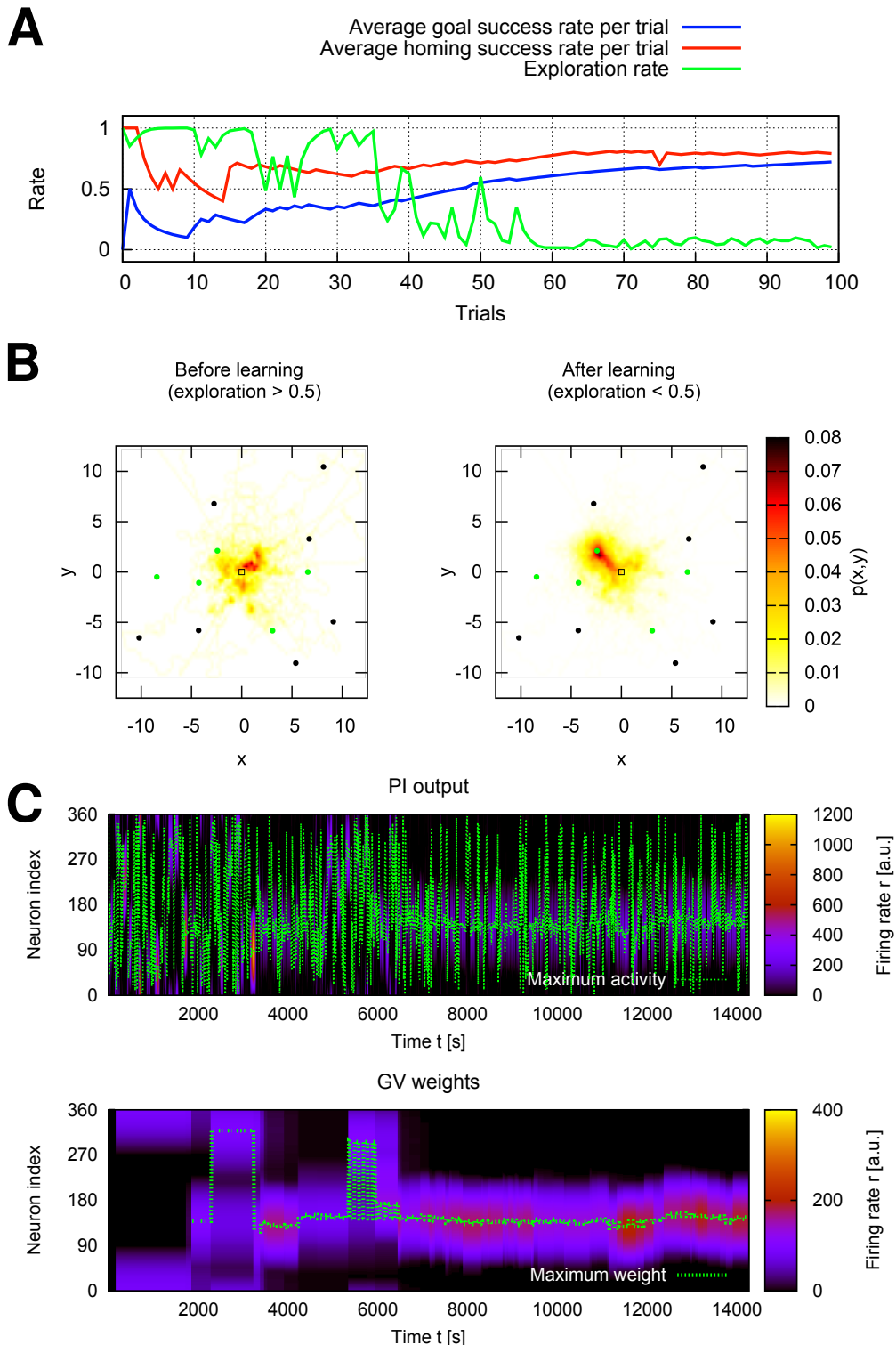


**Figure 4.6** Global vector learning results for 5% noise level. A) Success rates of goal reaching and homing, and exploration rate for 100 learning trials. B) Trajectory density maps before (left) and after learning (right). Visited goals during the experiments are indicated by green circles, while the black circles are the ones not visited by the agent. C) PI activities and GV weights with respect to time.

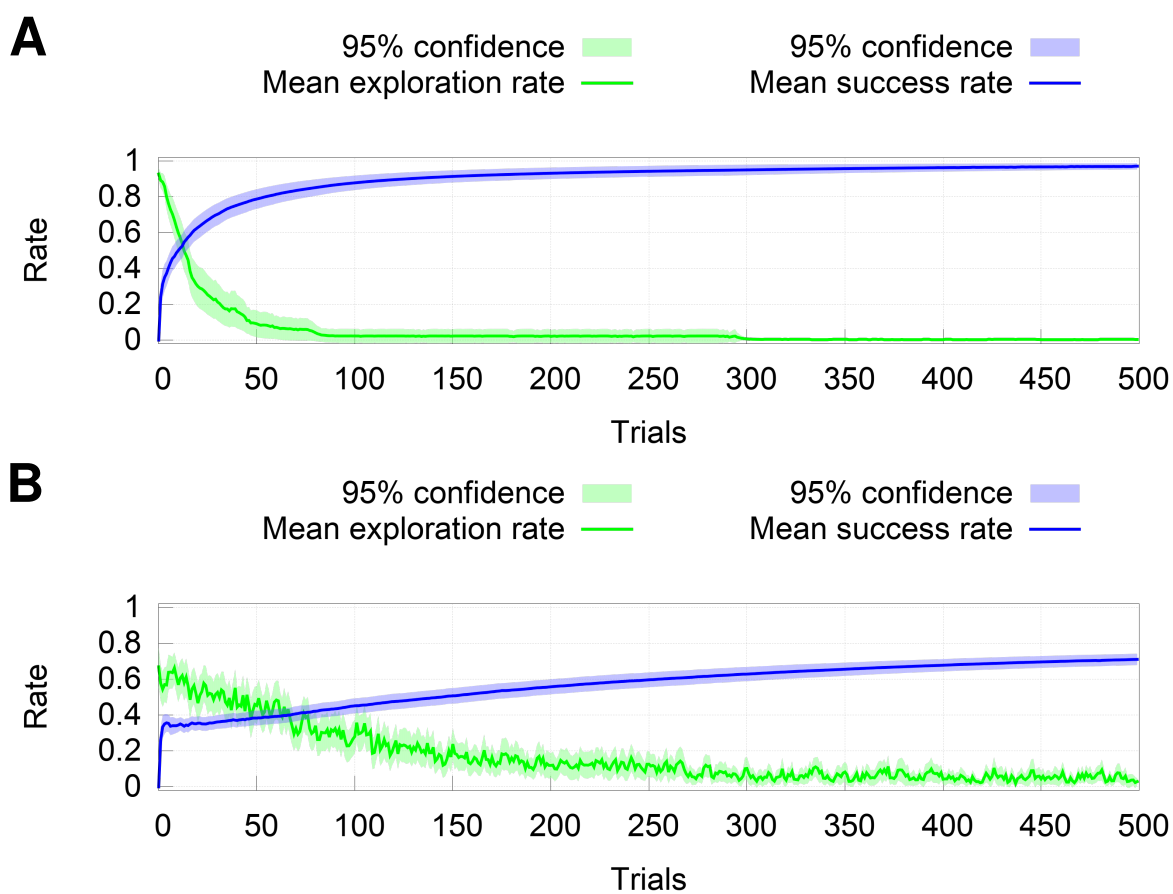


**Figure 4.7** Goal success rate and exploration rate with respect to the trial number averaged over 50 learning cycles with A) 0% sensory noise, and B) 5% sensory noise.

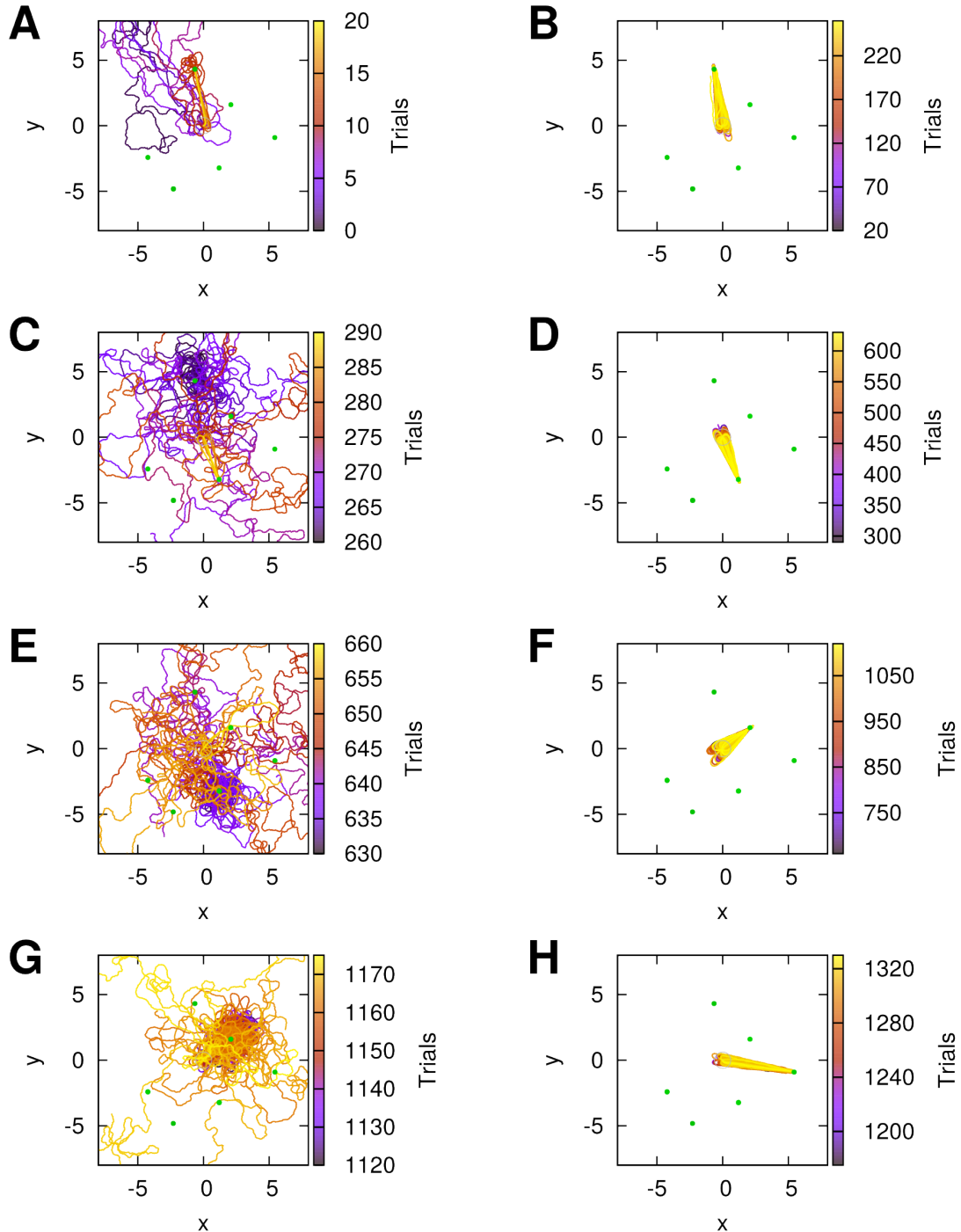


**Figure 4.8** Global vector learning in a dynamic environment with decaying rewards. A) Trials 0–20: The agent searches for goals and slowly learns the global vector  $(-0.64, 4.32)$ . B) Trials 20–260: The global vector is acquired and the exploration rate is close to zero. The amount of reward given decreases with every visit. C) Trials 260–290: When the reward reaches zero, the exploration rate increases. Thus, the agent randomly explores to learn other rewarding locations. D) Trials 290–630: A second global vector  $(1.21, -3.22)$  is learned and exploration rate is close to zero. Similar phases of subsequent extinction and acquisition of global vectors are shown for the trials E) 630–660, F) 660 – 1120, G) 1120–1175, and H) 1175–1330, respectively.

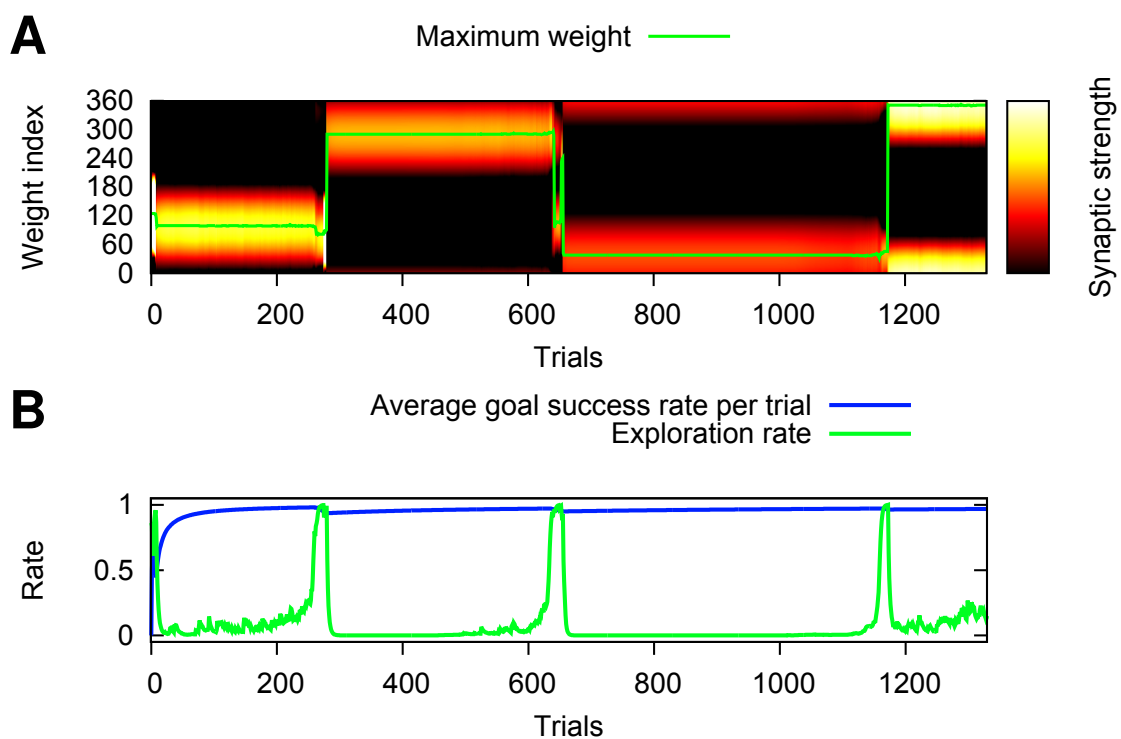


**Figure 4.9** Weights and rates during global vector learning in a dynamic environment. A) Synapses  $i$  to the GV array are shown with respect to trial number. The color coding of the heatmap corresponds to the synaptic strength  $W_i$ . The green-colored line indicates the maximum synaptic strength, which is equal to the direction to the learned goal. B) Exploration and success rate with respect to trial number. Exploration or searching phases are indicated by a high exploration rate. A global vector is acquired, when the exploration rate is low.

## CHAPTER 5

---

# MODULAR NEURAL ARCHITECTURE FOR DECISION MAKING IN SPATIAL NAVIGATION

---

*"Action is the real measure of intelligence."*

– Napoleon Hill (1883 - 1970)

### 5.1 Introduction

In order for insects to survive in dynamic environments, they need to select actions to maximize future rewards. In social insects, these actions may also have an influence on the survival of the colony. Experiments in foraging bumblebees have shown that the amount of nectar (feeding reward) has an effect on their behavior and action selection, and that they are able to associate predictive stimuli, such as the odor or the color of the flowers, with this reward (Dukas and Real, 1993; Real, 1981). Based on these experiments, Montague et al. (1995) presented a model based on predictive Hebbian learning. In their model, the agent receives visual input consisting of blue and yellow colored pixels. If the agent is near a flower, it receives a reward. Using temporal difference learning to adjust the agent's actions (directed flight or reorientation), Montague et al. (1995) show that their model created risk-aversive foraging behavior similar to what has been observed in the animals.

Inspired by these findings, this chapter presents an action selection mechanism that is applied in a foraging task similar to the ones described above. We extend our goal-based vector navigation control by a second learning circuit to allow for learning of multiple goals. Two types of goals (yellow & blue) are located in the environment. We assume that the agent is able to perceive the colors of the goals, which can be achieved by visual sensors. For simplicity, we use separate reward signals for both goals. The agent's task is to forage and learn the global vector for the two types of goals. Based on the experienced reward from both goals, the agent adjusts its decisions to navigate to one of the goals.

## 5.2 Static Action Choice for Two Goal Types

We extend the proposed learning circuit to learn vectors of the blue and yellow goals (see Fig. 5.1). During foraging, the agent learns global vectors of both the blue ( $B$ ) and yellow ( $Y$ ) goals based on their respective rewards.

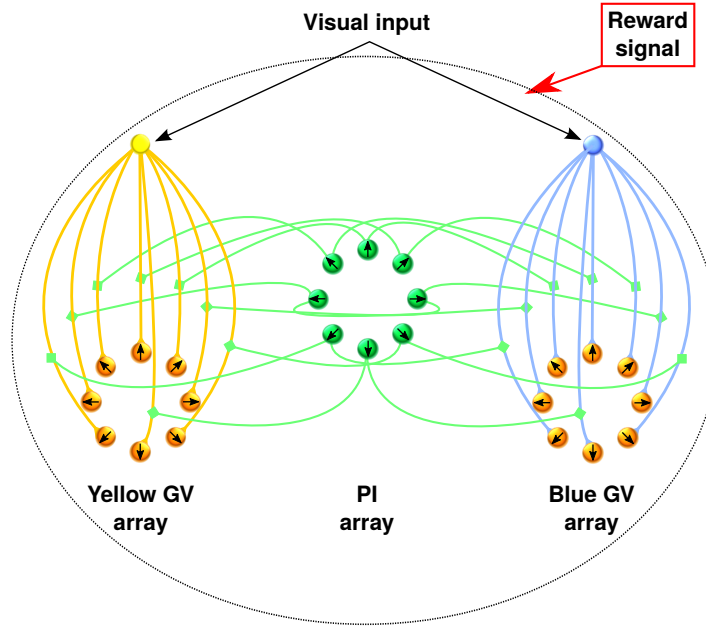


**Figure 5.1** A schematic of the extended learning circuit for multiple goals.

These rewards influence the agent's choice to move to either of the goals with probabilities given by the softmax distribution

$$p_B = \frac{\exp(\beta v_B)}{\exp(\beta v_B) + \exp(\beta v_Y)}, \quad (5.1)$$

$$p_Y = \frac{\exp(\beta v_Y)}{\exp(\beta v_B) + \exp(\beta v_Y)}, \quad (5.2)$$

where  $v_k = \sum_{i=0}^{t-1} \gamma^i r_k(i)$  is the value function for each of the goals  $k$ , and  $\beta$  is a parameter, which determines the responsiveness of the probabilities to the reward ratio  $r_B : r_Y$ . For large  $\beta$ , the probabilities diverge rapidly to 0 and 1, respectively. If  $\beta$  is small, the divergence rate is slower, such that decisions are random. Therefore, depending on the magnitude,  $\beta$  drives either exploration or exploitation in decision making.

The stochastic action choice

$$q = \begin{cases} B & \text{with prob. } p_B, \\ Y & \text{with prob. } p_Y, \end{cases} \quad (5.3)$$

is updated every 100 time steps, where

$$p_B + p_Y = 1. \quad (5.4)$$

Based on the choice  $q$ , the motor command is given by

$$m = |\mathbf{x}|(1 - \epsilon_q)m_{\text{hom}} + |\mathbf{y}|\xi(1 - \epsilon_q)m_{\text{goal}} + \epsilon_q\chi, \quad (5.5)$$

as defined as in Chapter 4, but here the exploration rate  $\epsilon_q$  is computed using the values  $v_q = \sum_{i=0}^{t-1} \gamma^i r_q(i)$  of the chosen goal.

### 5.3 Experimental Results

We carried out an experiment to demonstrate the decision making capabilities of the agent with varying parameters  $\beta$  and rewards  $r_B, r_Y$  given for each goal. The experiment lasted 400 trials and consisted of three phases with different values for  $\beta$ ,  $r_B$ , and  $r_Y$ . Fig. 5.2 shows the agent's trajectories for four subsequent intervals of trials. The experiment was initialized for the first 100 trials with  $\beta = 0.01$ ,  $r_B = 0.25$ , and  $r_Y = 1$ . Initially, the agent randomly explores the environment and learns global vectors. Given a small  $\beta$ , the choice probabilities adapt slowly towards choosing the yellow goal, which gives a higher reward. However, small  $\beta$  are required for learning of both global vectors. After 100 trials,  $\beta$  is increased to 1 and the probabilities rapidly shift the decisions towards the yellow goal. After 200 trials, we set the rewards to  $r_B = 0.75$  and  $r_Y = 0$ , thus, we reverse the reward bias. Because the agent does not receive any reward at the yellow goal, it changes its decision and navigates towards the blue goal. The agent performs shortcuts between the goals, which are achieved by the compensation of the current location using path integration. The reward received at the blue goal increases the choice probabilities for the blue goal. Finally, the agent navigates directly towards the blue goal.

Fig. 5.3 shows the exploration rates and accumulated visits of both goals, respectively. The results were average over 50 cycles of 400 trials. During the first 100 trials,  $\beta = 0.01$  leads to the acquisition of both global vectors. This is indicated by the decrease in exploration rate for both goals. When  $\beta = 1$ , the choice probabilities rapidly drift towards the higher rewarded, yellow goal. During this phase, the blue exploration rate is constant, because the agent decides to navigate only towards the yellow goal. After the reversal of rewards at trial 200, the agent adapts its decisions towards the blue goal. We would like to emphasize the importance of the initial learning of both global vectors given a small value of  $\beta$ . It allows for direct shortcuts from the yellow to the blue goal without the need of randomly exploring the environment.

### 5.4 Discussion

This chapter presented a reward-based mechanism for goal-directed decision making in artificial agents. The mechanism was inspired by a model by Montague et al. (1995), where bumblebee foraging was modelled using predictive Hebbian learning. We employed the idea of a stochastic policy based on experienced reward during foraging. As a result, the policy adapts to changes of rewards located in the environment. In a simple experimental setup consisting of two different goals with different rewards, we provide a proof-of-concept of decision making in an agent. It is important to emphasize that the results showed a behavior, in which the agent takes so-called novel shortcuts. These shortcuts allow to navigate from an unrewarded goal to another learned goal. This behavior has been observed in honeybees (Menzel et al., 2005), and it has further proved the concept of a cognitive map in honeybees. In contrast, our model has distributed spatial memories, which are not integrated into one shared representation. Similarly, Cruse and Wehner (2011) provided a model which can reproduce novel shortcuts without having a central integration of vector information. However, instead of providing a biological explanation of how global vectors are learned and in which context shortcircuiting behavior occurs, the authors focussed on disproving the "need of a cognitive map" for shortcircuiting behavior. On the contrary, our model provides a learning mechanism for global vectors, and the model presented in this chapter is a possible mechanism that might explain how the shortcircuiting behavior arises in foraging bees. In future

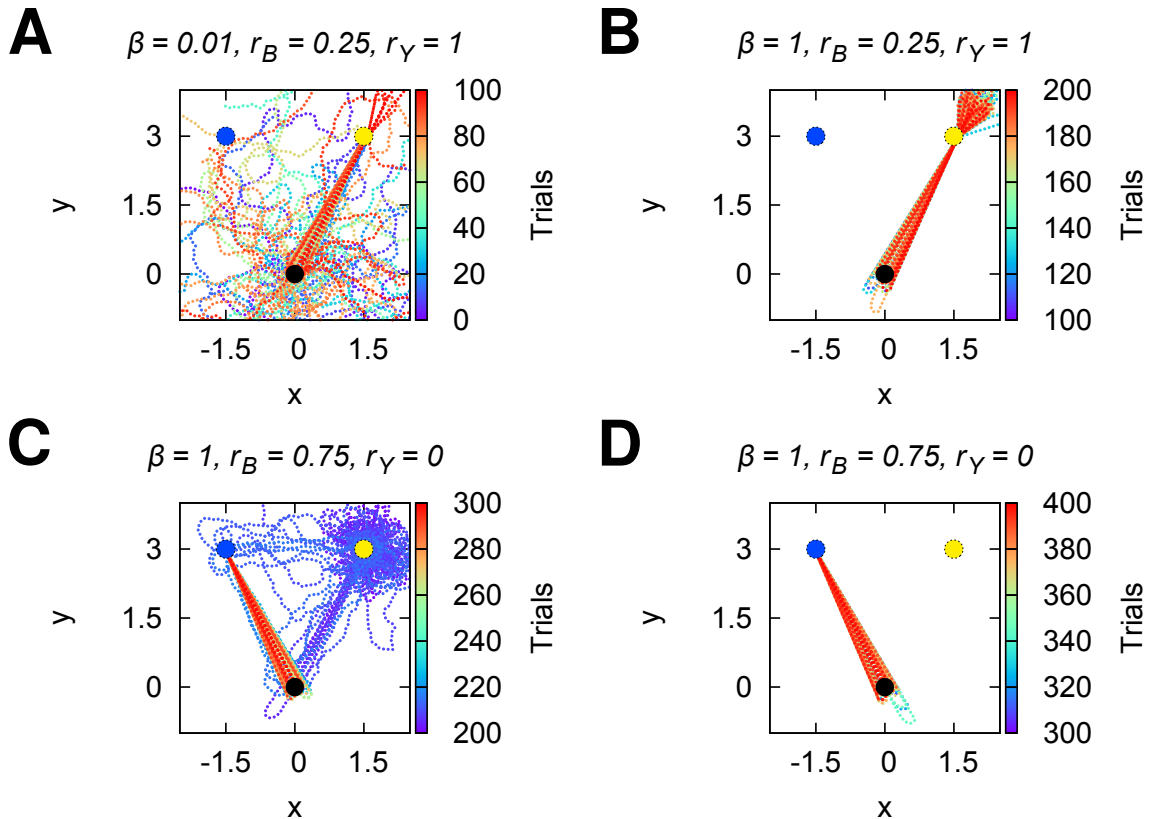


**Figure 5.2** Decision making of blue and yellow goals. The agent's trajectories are shown for four different phases of the experiment: A) 0–100, B) 100–200, C) 200–300, and D) 300–400 trials. See text for details.

work, we will extend the described decision-making mechanism with respect to insect foraging theories, e.g., optimal scale-free Lévy searches Reynolds (2008); Reynolds and Frye (2007); Viswanathan et al. (1999).

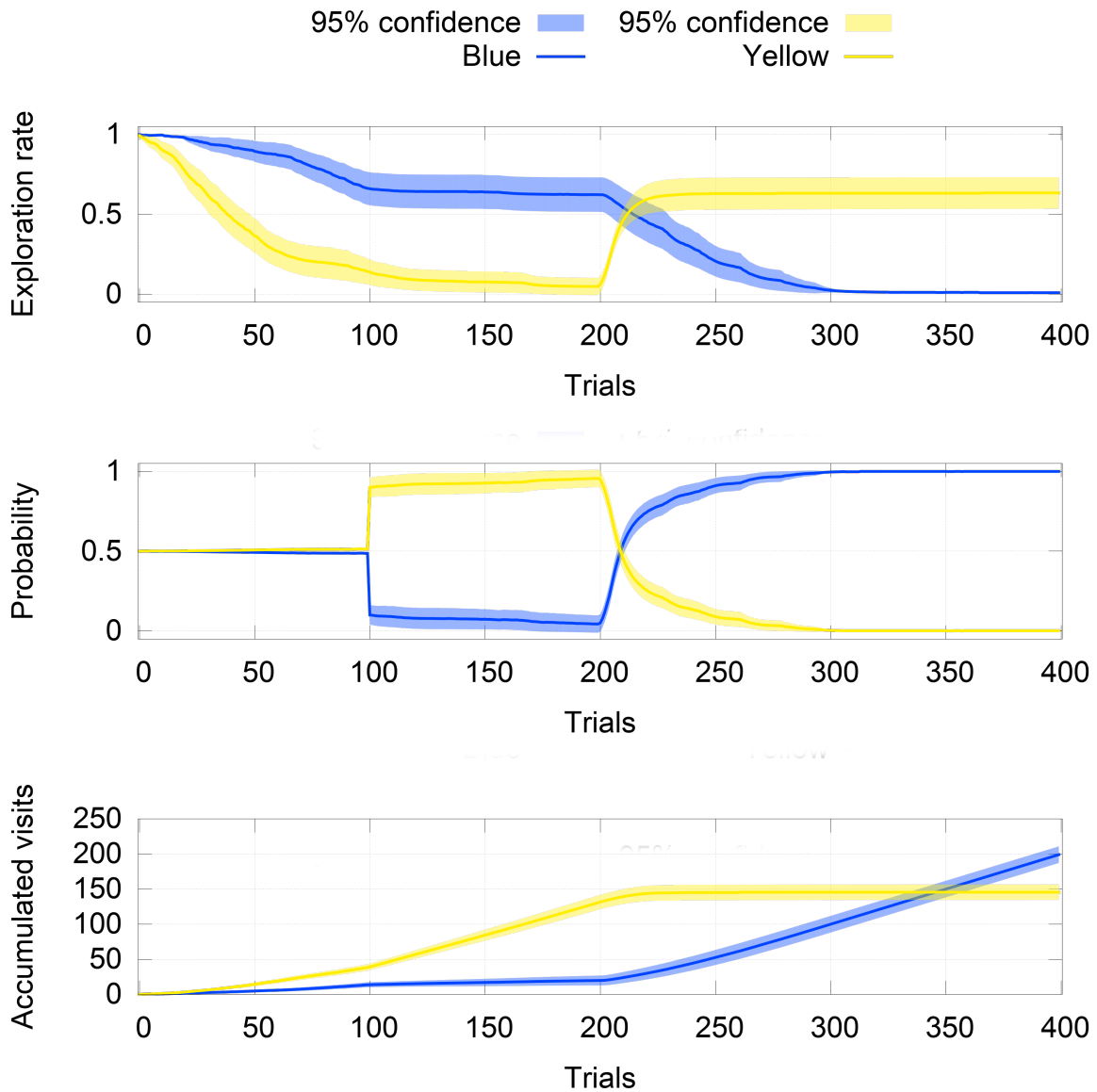


**Figure 5.3** Exploration rates, choice probabilities and sum of visits of blue and yellow goals in decision making. The measurements were averaged over 50 cycles.



## CHAPTER 6

---

## DISCUSSION

---

The goal of this thesis was to investigate insect-like adaptive navigation generated by a neural control architecture, and to implement such an architecture to an embodied legged agent. Animals achieve autonomous navigation in complex environments. Similarly, our control system allows for autonomous navigation as it was shown by the results of the previous Chapters 3, 4 and 5. Our control architecture consists of different modules that generate different behaviors similar to the ones observed in insect navigation, including *path integration*, *homing*, *foraging*, *searching*, *reward-based goal learning* and *goal-directed navigation* using *global vector memories*, as well as *goal-directed decision making*.

Insects exhibit remarkable capabilities in navigation. Interestingly, they achieve this level of performance by applying different behavioral strategies, which adaptively depend on the animal's experiences during navigation. Path integration, for example, is used by insects to form vector memories (Collett et al., 2013, 1998), which serve for goal-directed navigation (Collett et al., 1999). In a similar way, our model applies a reward-based associative learning rule to memorize vector information from the path integrator in an array of plastic synapses. To our knowledge, this combination of using path integration for reward-based vector learning in a biological plausible way has not been achieved. Hoinville et al. (2012) proposed a learning and memory mechanism to store vectors as  $x$  and  $y$  coordinates. However, this mechanism is not a plausible spatial representation in neural systems. Moreover, their mechanism does not account for the learning of new coordinates. In contrast to this, our model is able to forget global vectors and re-learn new ones. Flexibility of the global vector memories has also been observed in insects.

The learning rule applied in our model is based on rewards. During learning, the conditioned stimulus is associated with the reward. We applied a direct reward instead of a prediction error as it is used in the reinforcement learning models by Rescorla and Wagner (1972) and Sutton (1988). We applied the direct reward signal, because it leads to more stable learning during foraging experiments. The convergence of this learning

rule is achieved by the error term  $(x_i(n) - W_i(n))$ , which minimizes the mismatch between the home vector at the reward location and the global vector. Additional features of classical conditioning, such as extinction of conditioned stimuli are achieved by the vector mismatch. In preliminary tests, we applied an prediction error  $\delta = r - v$  using a normalized version of the previously defined value function (Eqn. 4.5). In future work, we aim to include prediction errors as a more biologically plausible reward signal in our learning rule.

As previously mentioned in Chapter 4, the maximum range of possibly learned goals is limited by the discount factor of the value function. A solution to this problem is to navigate towards the goal using landmarks for guidance. In fact, our learning circuit can be extended to allow for landmark-based route learning by adding a circular array as a local path integrator. The local path integrator is applied to learn local vectors, i.e. vectors with a locally defined origin, such as a landmark. In our model, these local vectors are learned recursively from the reward. Fig. 6.1 illustrates and explains how route learning is achieved by this proposed circuit. Because the learning of landmark-based vectors requires temporal sequence learning, we will apply temporal difference learning.

Although our control architecture generates insect-like adaptive vector navigation, it does not account for all behavioral aspects observed in insect navigation. Insects perform mainly visually-guided navigation (Srinivasan, 2010), our model does not depend on visual input. We restrict our approach to spatial learning of egocentric motion cues by means of path integration, because of the given scope of this thesis. Using only this spatial information does not limit our model from achieving insect-like spatial learning and navigation. However, we emphasize that visual sensors and visual processing could be added as an additional module for our architecture. This addition will be considered as future work. Other sensory modalities, such as olfactory and auditory sensors, could also be used to extend our control architecture. In particular, we will apply auditory sensors for localization of goals. Insects have an auditory system mediated by mechanoreceptors on the antennae (Robert and Göpfert, 2002). For example, parasitoid flies and wasps use their hearing for localization of host insects (Hedwig and Robert, 2014; Meyhöfer and Casas, 1999).

For more than fifty years, there has been a mutual relationship between neuroscience and computational modelling. Embodied agents, such as simulated or real-world robots, have been used as proof of concept for computational models as well as to test specific biological hypotheses. This thesis contributes to this field of study by presenting a behavior-based model of insect spatial behavior. This model is a step further towards the understanding of the behavioral organization and control mechanisms of learning and memory in insect navigation. Future applications of our model on insect-inspired mobile robots, such as hexapod robots and quadrocopters tested in real environments, could provide experimental platforms for behavioral hypotheses of insect navigation and learning.

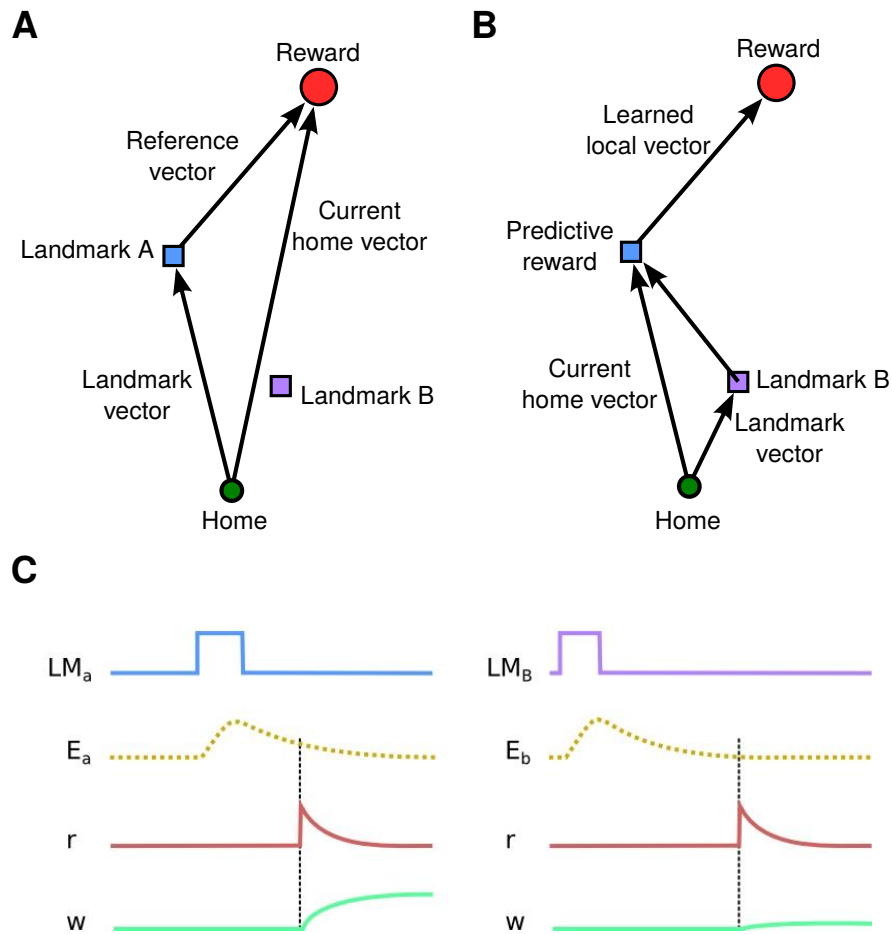


**Figure 6.1** A proposed scheme of recursive route learning. Top: Signals for learning landmarks closer to the reward (colors/numbers correspond to the bottom figure). Bottom: Recursive steps of route learning. Subsequent landmarks are learned by the predictive signal of the learned landmark. Symbols: LM, landmark; E, eligibility trace; r, reward signal; w, weight.



## Bibliography

---

- Adrian, E. and Zotterman, Y. (1926). The impulses produced by sensory nerve-endings: Part II. The response of a Single End-Organ. *The Journal of Physiology*, 61(2):151–171.
- Aihara, K., Takabe, T., and Toyoda, M. (1990). Chaotic neural networks. *Physics Letters A*, 144(6-7):333 – 340.
- Aksay, E., Gamkrelidze, G., Seung, H., Baker, R., and Tank, D. (2001). In vivo intracellular recording and perturbation of persistent activity in a neural integrator. *Nature neuroscience*, 4(2):184–193.
- Alves, C., Boal, J. G., and Dickel, L. (2008). Short-distance navigation in cephalopods: a review and synthesis. *Cognitive Processing*, 9(4):239–247.
- Anderson, C. H. and Van Essen, D. C. (1987). Shifter circuits: a computational strategy for dynamic aspects of visual processing. *Proceedings of the National Academy of Sciences*, 84(17):6297–6301.
- Arkin, R. C. (1989). Motor schema – based mobile robot navigation. *The International Journal of Robotics Research*, 8(4):92–112.
- Averbeck, B. B., Latham, P. E., and Pouget, A. (2006). Neural correlations, population coding and computation. *Nature reviews. Neuroscience*, 7(5):358–366.
- Beer, R. D. (1990). *Intelligence As Adaptive Behavior: An Experiment in Computational Neuroethology (Perspectives in Artificial Intelligence)*. Academic Press Professional.
- Bekey, G. A. (2005). *Autonomous robots: from biological inspiration to implementation and control*. MIT press.

- Bellman, R. (1952). On the theory of dynamic programming. *Proceedings of the National Academy of Sciences*, 38(8):716–719.
- Benhamou, S., Sauvé, J.-P., and Bovet, P. (1990). Spatial memory in large scale movements: Efficiency and limitation of the egocentric coding process. *Journal of Theoretical Biology*, 145(1):1 – 12.
- Bernardet, U., Bermúdez i Badia, S., and Verschure, P. F. M. J. (2008). A model for the neuronal substrate of dead reckoning and memory in arthropods: a comparative computational and behavioral study. *Theory in Biosciences*, 127(2):163–175.
- Bienenstock, E., Cooper, L., and Munro, P. (1982). Theory for the development of neuron selectivity: orientation specificity and binocular interaction in visual cortex. *The Journal of Neuroscience*, 2(1):32–48.
- Bisetzky, A. R. (1957). Die Tänze der Bienen nach einem Fussweg zum Futterplatz. *Zeitschrift für vergleichende Physiologie*, 40(3):264–288.
- Blum, M. and Labhart, T. (2000). Photoreceptor visual fields, ommatidial array, and receptor axon projections in the polarisation-sensitive dorsal rim area of the cricket compound eye. *Journal of Comparative Physiology A*, 186(2):119–128.
- Borenstein, J., Everett, H. R., Feng, L., and Wehe, D. (1997). Mobile robot positioning-sensors and techniques. Technical report, DTIC Document.
- Brooks, R. (1986). A robust layered control system for a mobile robot. *Robotics and Automation, IEEE Journal of*, 2(1):14–23.
- Burgess, N., Donnett, J. G., Jeffery, K. J., and O’Keefe, J. (1997). Robotic and neuronal simulation of the hippocampus and rat navigation. *Philosophical Transactions of the Royal Society of London. Series B: Biological Sciences*, 352(1360):1535–1543.
- Caianiello, E. (1961). Outline of a theory of thought-processes and thinking machines. *Journal of Theoretical Biology*, 1(2):204 – 235.
- Capaldi, E. A., Robinson, G. E., and Fahrbach, S. E. (1999). Neuroethology of spatial learning: The birds and the bees. *Annual Review of Psychology*, 50(1):651–682. PMID: 10074688.
- Cheung, A. (2014). Animal path integration: A model of positional uncertainty along tortuous paths. *Journal of Theoretical Biology*, 341(0):17 – 33.
- Cheung, A. and Vickerstaff, R. (2010). Finding the way with a noisy brain. *PLoS Comput Biol*, 6(11):e1000992.
- Chiel, H. J. and Beer, R. D. (1997). The brain has a body: adaptive behavior emerges from interactions of nervous system, body and environment. *Trends in Neurosciences*, 20(12):553 – 557.
- Collett, M., Chittka, L., and Collett, T. (2013). Spatial memory in insect navigation. *Current Biology*, 23(17):R789 – R800.
- Collett, M., Collett, T. S., Bisch, S., and Wehner, R. (1998). Local and global vectors in desert ant navigation. *Nature*, 394(6690):269–272.
- Collett, M., Collett, T. S., and Wehner, R. (1999). Calibration of vector navigation in desert ants. *Current Biology*, 9(18):1031 – S1.
- Collett, T. S. and Graham, P. (2004). Animal navigation: Path integration, visual landmarks and cognitive maps. *Current Biology*, 14(12):R475 – R477.

- Cruse, H. and Wehner, R. (2011). No need for a cognitive map: Decentralized memory for insect navigation. *PLoS Comput Biol*, 7(3):e1002009.
- Darwin, C. (1873). Origin of certain instincts. *Nature*, 7:417–418.
- De Marco, R. and Menzel, R. (2005). Encoding spatial information in the waggle dance. *Journal of Experimental Biology*, 208(20):3885–3894.
- de Perera, T. B. (2004). Fish can encode order in their spatial map. *Proceedings of the Royal Society of London. Series B: Biological Sciences*, 271(1553):2131–2134.
- Der, R. and Martius, G. (2012). *The playful machine*. Springer.
- Duelli, P. and Wehner, R. (1973). The spectral sensitivity of polarized light orientation in cataglyphis bicolor (formicidae, hymenoptera). *Journal of comparative physiology*, 86(1):37–53.
- Dukas, R. and Real, L. A. (1993). Effects of recent experience on foraging decisions by bumble bees. *Oecologia*, 94(2):244–246.
- Durrant-Whyte, H. and Bailey, T. (2006). Simultaneous localization and mapping: part i. *Robotics Automation Magazine, IEEE*, 13(2):99–110.
- Dyer, F. C. and Dickinson, J. A. (1994). Development of sun compensation by honeybees: how partially experienced bees estimate the sun's course. *Proceedings of the National Academy of Sciences*, 91(10):4471–4474.
- Elfes, A. (1989). Using occupancy grids for mobile robot perception and navigation. *Computer*, 22(6):46–57.
- Etienne, A. S. and Jeffery, K. J. (2004). Path integration in mammals. *Hippocampus*, 14(2):180–192.
- Eurich, C. W. and Schwegler, H. (1997). Coarse coding: calculation of the resolution achieved by a population of large receptive field neurons. *Biological Cybernetics*, 76(5):357–363.
- Fahrbach, S. E. (2006). Structure of the mushroom bodies of the insect brain. *Annual Review of Entomology*, 51(1):209–232. PMID: 16332210.
- Fent, K. and Wehner, R. (1985). Ocelli: A celestial compass in the desert ant cataglyphis. *Science*, 228(4696):192–194.
- Forel, A. (1902). Les fourmis du sahara algrien. *Ann. Soc. Ent. belgique*, 46:147 – 158.
- Franz, M. O. and Mallot, H. A. (2000). Biomimetic robot navigation. *Robotics and Autonomous Systems*, 30(1-2):133 – 153.
- Franz, M. O., Schölkopf, B., Mallot, H. A., and Bülthoff, H. H. (1998). Learning view graphs for robot navigation. In Bekey, G., editor, *Autonomous Agents*, pages 111–125. Springer US.
- Georgopoulos, A., Schwartz, A., and Kettner, R. (1986). Neuronal population coding of movement direction. *Science*, 233(4771):1416–1419.
- Görner, P. (1958). Die optische und kinästhetische Orientierung der Trichterspinne Agelena Labyrinthica (Cl.). *Zeitschrift für vergleichende Physiologie*, 41(2):111–153.
- Gould, J. L. (1998). Sensory bases of navigation. *Current Biology*, 8(20):R731 – R738.

- Grah, G., Wehner, R., and Ronacher, B. (2005). Path integration in a three-dimensional maze: ground distance estimation keeps desert ants *cataglyphis fortis* on course. *Journal of Experimental Biology*, 208(21):4005–4011.
- Gribakin, F., Vishnevskaya, T., and Polyanovskii, A. (1979). Polarization and spectral sensitivity of single photoreceptors of the domestic cricket. *Neurophysiology*, 11(5):358–365.
- Guo, P. and Ritzmann, R. E. (2013). Neural activity in the central complex of the cockroach brain is linked to turning behaviors. *The Journal of Experimental Biology*, 216(6):992–1002.
- Gurney, K., Prescott, T. J., Wickens, J. R., and Redgrave, P. (2004). Computational models of the basal ganglia: from robots to membranes. *Trends in Neurosciences*, 27(8):453 – 459.
- Haferlach, T., Wessnitzer, J., Mangan, M., and Webb, B. (2007). Evolving a neural model of insect path integration. *Adaptive Behavior*, 15(3):273–287.
- Hafting, T., Fyhn, M., Molden, S., Moser, M. B., and Moser, E. I. (2005). Microstructure of a spatial map in the entorhinal cortex. *Nature*, 436(7052):801–806.
- Hartmann, G. and Wehner, R. (1995). The ant's path integration system: a neural architecture. *Biological Cybernetics*, 73(6):483–497.
- Hebb, D. O. (1949). *The Organization of Behavior: A Neuropsychological Theory*. Wiley, New York, new ed edition.
- Hedwig, B. and Robert, D. (2014). Auditory parasitoid flies exploiting acoustic communication of insects. In Hedwig, B., editor, *Insect Hearing and Acoustic Communication*, volume 1 of *Animal Signals and Communication*, pages 45–63. Springer Berlin Heidelberg.
- Heinrich, B. (1984). Learning in invertebrates. In Marler, P. and Terrace, H., editors, *The Biology of Learning*, volume 29 of *Dahlem Workshop Reports*, pages 135–147. Springer Berlin Heidelberg.
- Heinze, S. and Homberg, U. (2007). Maplike representation of celestial e-vector orientations in the brain of an insect. *Science*, 315(5814):995–997.
- Hertz, J., Palmer, R. G., and Krogh, A. S. (1991). *Introduction to the Theory of Neural Computation*. Addison-Wesley Publishing Company, 1st edition.
- Hoinville, T., Wehner, R., and Cruse, H. (2012). Learning and retrieval of memory elements in a navigation task. In Prescott, T., Lepora, N., Mura, A., and Verschure, P., editors, *Biomimetic and Biohybrid Systems*, volume 7375 of *Lecture Notes in Computer Science*, pages 120–131. Springer Berlin Heidelberg.
- Homberg, U., Heinze, S., Pfeiffer, K., Kinoshita, M., and el Jundi, B. (2011). Central neural coding of sky polarization in insects. *Philosophical Transactions of the Royal Society B: Biological Sciences*, 366(1565):680–687.
- Hopfield, J. (1984). Neurons with graded response have collective computational properties like those of two-state neurons. *Proceedings of the National Academy of Sciences of the United States of America*, 81(10):3088–3092.
- Hubel, D. H. and Wiesel, T. N. (1959). Receptive fields of single neurones in the cat's striate cortex. *The Journal of Physiology*, 148(3):574–591.
- Jacobs, G. A., Miller, J. P., and Aldworth, Z. (2008). Computational mechanisms of mechanosensory processing in the cricket. *Journal of Experimental Biology*, 211(11):1819–1828.

- Jander, R. (1957). Die optische Richtungsorientierung der Roten Waldameise (*Formica Rufa L.*). *Zeitschrift für vergleichende Physiologie*, 40(2):162–238.
- Jozet-Alves, C., Darmillacq, A.-S., and Boal, J. G. (2014). *Navigation in cephalopods*, chapter 7, pages 150 – 176. Cephalopod Cognition. Cambridge University Press.
- Khatib, O. (1985). The potential field approach and operational space formulation in robot control. In *Proc. of the 4th Yale Workshop on Applications of Adaptive Systems Theory*, pages 208–214, Yale University, New Haven, CT, USA.
- Kim, D. and Lee, J. (2011). Path integration mechanism with coarse coding of neurons. *Neural Processing Letters*, 34(3):277–291.
- Kim, D. E. and Hallam, J. C. (2000). Neural network approach to path integration for homing navigation. In *From Animals to Animats 6: Proceedings of the Sixth International Conference on Simulation of Adaptive Behavior*, volume 6, page 228. Fordham Univ Press.
- Kramer, G. (1952). Experiments on bird orientation. *Ibis*, 94(2):265–285.
- Labhart, T. (1988). Polarization-opponent interneurons in the insect visual system. *Nature*, 331(6155):435–437.
- Labhart, T. and Meyer, E. P. (2002). Neural mechanisms in insect navigation: polarization compass and odometer. *Current Opinion in Neurobiology*, 12(6):707 – 714.
- Lambrinos, D., Möller, R., Labhart, T., Pfeifer, R., and Wehner, R. (2000). A mobile robot employing insect strategies for navigation. *Robotics and Autonomous Systems*, 30(12):39 – 64.
- Laurent, G. and Davidowitz, H. (1994). Encoding of olfactory information with oscillating neural assemblies. *Science*, 265(5180):1872–1875.
- Manoonpong, P., Geng, T., Kulvicius, T., Porr, B., and Wörgötter, F. (2007). Adaptive, fast walking in a biped robot under neuronal control and learning. *PLoS Comput Biol*, 3(7):e134.
- Manoonpong, P., Parlitz, U., and Wörgötter, F. (2013). Neural control and adaptive neural forward models for insect-like, energy-efficient, and adaptable locomotion of walking machines. *Frontiers in Neural Circuits*, 7(12).
- Markl, H. (1962). Borstenfelder an den Gelenken als Schweresinnesorgane bei Ameisen und anderen Hymenopteren. *Zeitschrift für vergleichende Physiologie*, 45(5):475–569.
- Martin, J.-R., Ernst, R., and Heisenberg, M. (1998). Mushroom Bodies Suppress Locomotor Activity in *Drosophila melanogaster*. *Learning & Memory*, 5(1):179–191.
- Maurer, R. and Séguinot, V. (1995). What is modelling for? a critical review of the models of path integration. *Journal of Theoretical Biology*, 175(4):457 – 475.
- McCulloch, W. and Pitts, W. (1943). A logical calculus of the ideas immanent in nervous activity. *The bulletin of mathematical biophysics*, 5(4):115–133.
- McGuire, S. E., Le, P. T., and Davis, R. L. (2001). The Role of *Drosophila* Mushroom Body Signaling in Olfactory Memory. *Science*, 293(5533):1330–1333.
- Menzel, R. (1987). Memory traces in honeybees. In Menzel, R. and Mercer, A., editors, *Neurobiology and Behavior of Honeybees*, pages 310–325. Springer Berlin Heidelberg.

- Menzel, R., Greggers, U., Smith, A., Berger, S., Brandt, R., Brunke, S., Bundrock, G., Hlse, S., Plmpe, T., Schaupp, F., Schttler, E., Stach, S., Stindt, J., Stollhoff, N., and Watzl, S. (2005). Honey bees navigate according to a map-like spatial memory. *Proceedings of the National Academy of Sciences of the United States of America*, 102(8):3040–3045.
- Menzel, R. and Muller, U. (1996). Learning and memory in honeybees: From behavior to neural substrates. *Annual Review of Neuroscience*, 19(1):379–404. PMID: 8833448.
- Merlin, C., Geegar, R. J., and Reppert, S. M. (2009). Antennal circadian clocks coordinate sun compass orientation in migratory monarch butterflies. *Science*, 325(5948):1700–1704.
- Meyhöfer, R. and Casas, J. (1999). Vibratory stimuli in host location by parasitic wasps. *Journal of Insect Physiology*, 45(11):967 – 971.
- Milford, M. and Wyeth, G. (2008). Mapping a suburb with a single camera using a biologically inspired slam system. *Robotics, IEEE Transactions on*, 24(5):1038–1053.
- Milford, M., Wyeth, G., and Prasser, D. (2004). RatSLAM: a hippocampal model for simultaneous localization and mapping. In *Robotics and Automation, 2004. Proceedings. ICRA '04. 2004 IEEE International Conference on*, volume 1, pages 403–408 Vol.1.
- Mittelstaedt, H. (1962). Control systems of orientation in insects. *Annual Review of Entomology*, 7(1):177–198.
- Mittelstaedt, H. (1983). The role of multimodal convergence in homing by path integration. *Fortschritte der Zoologie*, 28:197 – 212.
- Mittelstaedt, H. and Mittelstaedt, M.-L. (1982). Homing by path integration. In Papi, F. and Wallraff, H., editors, *Avian Navigation, Proceedings in Life Sciences*, pages 290–297. Springer Berlin Heidelberg.
- Mittelstaedt, M.-L. and Glasauer, S. (1991). Idiothetic navigation in gerbils and humans. *Zool. Jb. Physiol*, 95(427-435).
- Mittelstaedt, M.-L. and Mittelstaedt, H. (1980). Homing by path integration in a mammal. *Naturwissenschaften*, 67(11):566–567.
- Mizunami, M. (1995). Functional diversity of neural organization in insect ocellar systems. *Vision Research*, 35(4):443 – 452.
- Mizunami, M., Weibrech, J. M., and Strausfeld, N. J. (1998). Mushroom bodies of the cockroach: their participation in place memory. *Journal of Comparative Neurology*, 402(4):520–537.
- Möller, R. (2012). A model of ant navigation based on visual prediction. *Journal of Theoretical Biology*, 305(0):118 – 130.
- Montague, P. R., Dayan, P., Person, C., and Sejnowski, T. J. (1995). Bee foraging in uncertain environments using predictive hebbian learning. *Nature*, 377(6551):725–728.
- Mote, M. and Wehner, R. (1980). Functional characteristics of photoreceptors in the compound eye and ocellus of the desert ant, cataglyphis bicolor. *Journal of comparative physiology*, 137(1):63–71.
- Mudra, R. and Douglas, R. J. (2003). Self-correction mechanism for path integration in a modular navigation system on the basis of an egocentric spatial map. *Neural Networks*, 16(9):1373 – 1388. Neuroinformatics.
- Müller, M. and Wehner, R. (1988). Path integration in desert ants, cataglyphis fortis. *Proceedings of the National Academy of Sciences*, 85(14):5287–5290.

- Müller, M. and Wehner, R. (2010). Path integration provides a scaffold for landmark learning in desert ants. *Current Biology*, 20(15):1368 – 1371.
- Murphy, J. J. (1873). Instinct: A mechanical analogy. *Nature*, 7:483.
- Nagumo, J. and Sato, S. (1972). On a response characteristic of a mathematical neuron model. *Kybernetik*, 10(3):155–164.
- Neuser, K., Triphan, T., Mronz, M., Poeck, B., and Strauss, R. (2008). Analysis of a spatial orientation memory in Drosophila. *Nature*, 453(7199):1244–1247.
- Ofstad, T. A., Zuker, C. S., and Reiser, M. B. (2011). Visual place learning in Drosophila melanogaster. *Nature*, 474(7350):204–207.
- Oja, E. (1982). Simplified neuron model as a principal component analyzer. *Journal of Mathematical Biology*, 15(3):267–273.
- O’Keefe, J. and Dostrovsky, J. (1971). The hippocampus as a spatial map. preliminary evidence from unit activity in the freely-moving rat. *Brain Research*, 34(1):171 – 175.
- O’Keefe, J. and Nadel, L. (1978). *The hippocampus as a cognitive map*, volume 3. Clarendon Press Oxford.
- Pasemann, F. (1993). Dynamics of a single model neuron. *International Journal of Bifurcation and Chaos*, 03(02):271–278.
- Pasemann, F. (1997). A simple chaotic neuron. *Physica D: Nonlinear Phenomena*, 104(2):205 – 211.
- Pasemann, F. (1999). Synchronizing chaotic neuromodules. In *European Symposium on Artificial Neural Networks (ESANN 1999)*.
- Pasemann, F., Rempis, C., and von Twickel, A. (2012). Evolving humanoid behaviors for language games. In Steels, L. and Hild, M., editors, *Language Grounding in Robots*, pages 67–86. Springer US.
- Pavlov, I. (1927). *Conditioned Reflexes: An Investigation of the Physiological Activity of the Cerebral Cortex*. Oxford University Press.
- Pfeifer, R., Lungarella, M., and Iida, F. (2007). Self-organization, embodiment, and biologically inspired robotics. *Science*, 318(5853):1088–1093.
- Pfeiffer, K. and Homberg, U. (2014). Organization and functional roles of the central complex in the insect brain. *Annual Review of Entomology*, 59(1):165–184. PMID: 24160424.
- Porr, B. and Wörgötter, F. (2006). Strongly improved stability and faster convergence of temporal sequence learning by utilising input correlations only. *Neural Computation*, 18(6):1380–1412.
- Prescott, T. J. (1996). Spatial representation for navigation in animats. *Adaptive Behavior*, 4(2):85–123.
- Real, L. A. (1981). Uncertainty and pollinator-plant interactions: The foraging behavior of bees and wasps on artificial flowers. *Ecology*, 62(1):pp. 20–26.
- Rescorla, R. A. and Wagner, A. W. (1972). *A theory of Pavlovian conditioning: Variations in the effectiveness of reinforcement and nonreinforcement*, chapter 3, pages 64–99. Appleton-Century-Crofts, New York.
- Reynolds, A. M. (2008). Optimal random Lévy-loop searching: New insights into the searching behaviours of central-place foragers. *EPL (Europhysics Letters)*, 82(2):20001.

- Reynolds, A. M. and Frye, M. A. (2007). Free-Flight Odor Tracking in *Drosophila* Is Consistent with an Optimal Intermittent Scale-Free Search. *PLoS ONE*, 2(4):e354.
- Riley, J., Greggers, U., Smith, A., Reynolds, D., and Menzel, R. (2005). The flight paths of honeybees recruited by the waggle dance. *Nature*, 435(7039):205–207.
- Robert, D. and Göpfert, M. C. (2002). Novel schemes for hearing and orientation in insects. *Current Opinion in Neurobiology*, 12(6):715 – 720.
- Rosenblatt, F. (1962). *Principles of neurodynamics: perceptrons and the theory of brain mechanisms*. Report (Cornell Aeronautical Laboratory). Spartan Books.
- Santschi, F. (1911). Observations et remarques critiques sur le mecanisme de l'orientation chez les fourmis. *Rev Suisse Zool*, 19:303 – 338.
- Schmid-Hempel, P. (1984). Individually different foraging methods in the desert ant *cataglyphis bicolor* (hy-menoptera, formicidae). *Behavioral Ecology and Sociobiology*, 14(4):263–271.
- Seelig, J. D. and Jayaraman, V. (2013). Feature detection and orientation tuning in the *Drosophila* central complex. *Nature*, 503(7475):262–266.
- Séguinot, V., Cattet, J., and Benhamou, S. (1998). Path integration in dogs. *Animal Behaviour*, 55(4):787 – 797.
- Sejnowski, T. J. and Tesauro, G. (1989). The Hebb rule for synaptic plasticity: algorithms and implementations. *Neural models of plasticity: Experimental and theoretical approaches*, pages 94–103.
- Sharpe, T. and Webb, B. (1998). Simulated and situated models of chemical trail following in ants. In *Proc. 5th Int. Conf. Simulation of Adaptive Behavior*, pages 195–204.
- Sinsch, U. (2006). Orientation and navigation in amphibia. *Marine and Freshwater Behaviour and Physiology*, 39(1):65–71.
- Skinner, B. F. (1938). The behavior of organisms: An experimental analysis.
- Softky, W. R. (1996). Fine analog coding minimizes information transmission. *Neural Networks*, 9(1):15 – 24.
- Srinivasan, M. (2014). Going with the flow: a brief history of the study of the honeybees navigational odometer. *Journal of Comparative Physiology A*, 200(6):563–573.
- Srinivasan, M., Zhang, S., and Bidwell, N. (1997). Visually mediated odometry in honeybees. *The Journal of Experimental Biology*, 200(19):2513–22.
- Srinivasan, M. V. (2010). Honey bees as a model for vision, perception, and cognition. *Annual Review of Entomology*, 55(1):267–284. PMID: 19728835.
- Steingrube, S., Timme, M., Wörgötter, F., and Manoonpong, P. (2010). Self-organized adaptation of a simple neural circuit enables complex robot behaviour. *Nature Physics*, 6(3):224–230.
- Strausfeld, N., Hansen, L., Li, Y., Gomez, R., and Ito, K. (1998). Evolution, discovery, and interpretations of arthropod mushroom bodies. *Learning & memory (Cold Spring Harbor, N.Y.)*, 5(1-2):1–37.
- Strausfeld, N. J. and Hirth, F. (2013). Deep homology of arthropod central complex and vertebrate basal ganglia. *Science*, 340(6129):157–161.
- Strauss, R. (2002). The central complex and the genetic dissection of locomotor behaviour. *Current Opinion in Neurobiology*, 12(6):633 – 638.

- Strauss, R. (2014). Neurobiological models of the central complex and the mushroom bodies. In Arena, P. and Patan, L., editors, *Spatial Temporal Patterns for Action-Oriented Perception in Roving Robots II*, volume 21 of *Cognitive Systems Monographs*, pages 3–41. Springer International Publishing.
- Strauss, R., Hanesch, U., Kinkelin, M., Wolf, R., and Heisenberg, M. (1992). No-Bridge of Drosophila Melanogaster: Portrait of a Structural Brain Mutant of the Central Complex. *Journal of Neurogenetics*, 8(3):125–155.
- Strauss, R. and Pichler, J. (1998). Persistence of orientation toward a temporarily invisible landmark in *Drosophila melanogaster*. *Journal of Comparative Physiology A*, 182(4):411–423.
- Strösslin, T., Sheynikhovich, D., Chavarriaga, R., and Gerstner, W. (2005). Robust self-localisation and navigation based on hippocampal place cells. *Neural Networks*, 18(9):1125 – 1140. Computational Theories of the Functions of the Hippocampus.
- Sutton, R. S. (1988). Learning to predict by the methods of temporal differences. *Machine Learning*, 3(1):9–44.
- Sutton, R. S. and Barto, A. G. (1998). *Introduction to Reinforcement Learning*. MIT Press, Cambridge, MA, USA, 1st edition.
- Szyszka, P., Galkin, A., and Menzel, R. (2008). Associative and non-associative plasticity in kenyon cells of the honeybee mushroom body. *Frontiers in Systems Neuroscience*, 2(3).
- Taube, J., Müller, R., and Ranck, J. (1990). Head-direction cells recorded from the postsubiculum in freely moving rats. i. description and quantitative analysis. *The Journal of Neuroscience*, 10(2):420–435.
- Thrun, S. and Leonard, J. J. (2008). Simultaneous localization and mapping. *Springer handbook of robotics*, pages 871–889.
- Tolman, E. C. (1948). Cognitive maps in rats and man. *Psychological Review*, 55:189–208.
- Touretzky, D., Redish, A., and Wan, H. (1993). Neural representation of space using sinusoidal arrays. *Neural Computation*, 5(6):869–884.
- Träger, U. and Homberg, U. (2011). Polarization-sensitive descending neurons in the locust: Connecting the brain to thoracic ganglia. *The Journal of Neuroscience*, 31(6):2238–2247.
- Trullier, O., Wiener, S. I., Berthoz, A., and Meyer, J.-A. (1997). Biologically based artificial navigation systems: Review and prospects. *Progress in Neurobiology*, 51(5):483 – 544.
- Vickerstaff, R. J. and Cheung, A. (2010). Which coordinate system for modelling path integration? *Journal of Theoretical Biology*, 263(2):242 – 261.
- Viswanathan, G., Buldyrev, S. V., Havlin, S., Da Luz, M., Raposo, E., and Stanley, H. E. (1999). Optimizing the success of random searches. *Nature*, 401(6756):911–914.
- von Frisch, K. (1949). Die Polarisation des Himmelslichtes als orientierender Faktor bei den Tänzen der Bienen. *Experientia*, 5(4):142–148.
- von Frisch, K. (1950). Die Sonne als Kompaß im Leben der Bienen. *Experientia*, 6(6):210–221.
- von Frisch, K. (1965). *Tanzsprache und Orientierung der Bienen*. Springer Verlag.
- von Holst, E. (1950). Die Arbeitsweise des Statolithenapparates bei Fischen. *Zeitschrift für vergleichende Physiologie*, 32(1-2):60–120.

- von Philipsborn, A. and Labhart, T. (1990). A behavioural study of polarization vision in the fly, *musca domestica*. *Journal of Comparative Physiology A*, 167(6):737–743.
- von Saint Paul, U. (1982). Do geese use path integration for walking home? In Papi, F. and Wallraff, H. G., editors, *Avian Navigation, Proceedings in Life Sciences*, pages 298–307. Springer Berlin Heidelberg.
- Walter, W. G. (1953). *The living brain*. WW Norton.
- Wang, X.-J. (2001). Synaptic reverberation underlying mnemonic persistent activity. *Trends in Neurosciences*, 24(8):455 – 463.
- Wehner, R. (1984). Astronavigation in insects. *Annual Review of Entomology*, 29(1):277–298.
- Wehner, R. (2003). Desert ant navigation: how miniature brains solve complex tasks. *Journal of Comparative Physiology A*, 189(8):579–588.
- Wehner, R. and Wehner, S. (1986). Path integration in desert ants. approaching a long-standing puzzle in insect navigation. *Monitore Zoologico Italiano - Italian Journal of Zoology*, 20(3):309–331.
- Weir, P. T., Schnell, B., and Dickinson, M. H. (2014). Central complex neurons exhibit behaviorally gated responses to visual motion in *Drosophila*. *Journal of Neurophysiology*, 111(1):62–71.
- Wintergerst, S. and Ronacher, B. (2012). Discrimination of inclined path segments by the desert ant *Cataglyphis fortis*. *Journal of Comparative Physiology A*, 198(5):363–373.
- Wittlinger, M., Wehner, R., and Wolf, H. (2006). The ant odometer: Stepping on stilts and stumps. *Science*, 312(5782):1965–1967.
- Wittlinger, M., Wehner, R., and Wolf, H. (2007). The desert ant odometer: a stride integrator that accounts for stride length and walking speed. *Journal of Experimental Biology*, 210(2):198–207.
- Wittmann, T. and Schwiegler, H. (1995). Path integration – a network model. *Biological Cybernetics*, 73(6):569–575.
- Wystrach, A. and Graham, P. (2012). What can we learn from studies of insect navigation? *Animal Behaviour*, 84(1):13 – 20.
- Zars, T., Fischer, M., Schulz, R., and Heisenberg, M. (2000). Localization of a Short-Term Memory in *Drosophila*. *Science*, 288(5466):672–675.
- Zeil, J. (1998). Homing in fiddler crabs (*Uca lactea annulipes* and *Uca vomeris*: Ocypodidae). *Journal of Comparative Physiology A*, 183(3):367–377.
- Zeil, J., Boeddeker, N., and Stürzl, W. (2010). Visual homing in insects and robots. In Floreano, D., Zufferey, J.-C., Srinivasan, M. V., and Ellington, C., editors, *Flying Insects and Robots*, pages 87–100. Springer Berlin Heidelberg.

## APPENDIX A

### NAVISIM

---

**NaviSim** is a C++-based simulation of a moving point (agent) in a two-dimensional environment. The kinematics of the point agent are described by continuous-time updates of linear displacements defined by the moving speed in a particular direction

$$\Delta x(t) = \Delta s(t) \cos(\phi(t)) \quad (\text{A.1})$$

$$\Delta y(t) = \Delta s(t) \sin(\phi(t)) \quad (\text{A.2})$$

$$\Delta s(t) = v \Delta t \quad (\text{A.3})$$

where  $dt = 0.1$  s is the integration interval. The speed  $v$  is assumed to be constant for this time interval. The motor command  $m_\phi$  from the controller determines the change in heading orientation  $\frac{d\phi}{dt} = m_\phi$  of the agent.

The class structure is designed in a modular way, in which several classes handle environment (e.g., agents, goals, landmarks) and control modules as described in this thesis. NaviSim is an open-source project and available under <https://github.com/degoldcode/NaviSim>.



## APPENDIX B

### LPZROBOTS

---

The open-source robot simulator *Lpzrobots* (see <https://github.com/georgmartius/lpzrobots>) based on the Open Dynamics Engine (ODE) is used to simulate AMOS II and to test the developed control architecture. *Lpzrobots* was developed by a collaboration of several research groups including *Neuroinformatics and Robotics* at the University of Leipzig and *Self-organization in Adaptive Systems* at the Max Planck Institute (MPI) for Dynamics and Self-organization in Göttingen. For experimental purposes, *AMOS II* has been simulated using *Lpzrobots*. The simulated version has the same properties as the real model. The programming interface of robots is determined by robot, simulation and controller files. We used *Eclipse* as an interface for programming *Lpzrobots* simulations in C++ along with an EGit plug-in for Git version control. For details of the simulation of *AMOS II*, please visit <https://github.com/georgmartius/lpzrobots>. The simulation provides possibilities to control and display certain parameters via console and *guilogger*.



## APPENDIX C

### AMOS II

---

*AMOS II* is a biologically inspired hexapod robot developed to study neural control of locomotion of living creatures. The robot body is inspired by the morphology of cockroaches. Its six identical legs are connected to the trunk which consists of two thoracic, jointed segments. Body flexibility is assured by an active backbone joint. In addition, an active tail can be attached to the rear part of the robot. In contrast to biological systems, body movements of *AMOS II* are controlled by a joint servomotor. Each leg has three joints (three DOF). The TC joint controls forward/backward motion of the leg, the CTr joint has the role of extension and flexion of the second limb and the motion of the third limb (up and down) is driven by the FTi joint. Besides the motors, *AMOS II* has 33 sensors for perceiving its environment: nineteen joint angle sensors, six foot contact sensors, eight infrared (IR) sensors (two at the front of the trunk and six located at the front of each leg). All in all, these sensors and motors are deployed for generating various behaviors (e.g., obstacle avoidance, escape responses, phototaxis).

